

This discussion paper is/has been under review for the journal Atmospheric Chemistry and Physics (ACP). Please refer to the corresponding final paper in ACP if available.

Nitrogen speciation in various types of aerosol in spring over the northwestern Pacific Ocean

L. Luo¹, X. H. Yao², H. W. Gao², S. C. Hsu³, J. W. Li⁴, and S.-J. Kao¹

¹State Key Laboratory of Marine Environmental Science, Xiamen University, Xiamen 361102, China

²Key Lab of Marine Environmental Science and Ecology, Ministry of Education, Ocean University of China, Qingdao 266100, China

³Research Center for Environmental Changes, Academia Sinica, Taipei, Taiwan

⁴Key Laboratory of Regional Climate-Environment for Temperate East Asia (RCE-TEA), Institute of Atmospheric Physics (IAP), Chinese Academy of Sciences (CAS), Beijing 100029, China

Received: 25 June 2015 – Accepted: 21 August 2015 – Published: 18 September 2015

Correspondence to: S.-J. Kao (sjkao@xmu.edu.cn)

Published by Copernicus Publications on behalf of the European Geosciences Union.

ACPD

15, 25583–25625, 2015

Nitrogen speciation
in various types of
aerosol in spring over
the northwestern
Pacific Ocean

L. Luo et al.

[Title Page](#)

[Abstract](#)

[Introduction](#)

[Conclusions](#)

[References](#)

[Tables](#)

[Figures](#)

[|◀](#)

[▶|](#)

[◀](#)

[▶](#)

[Back](#)

[Close](#)

[Full Screen / Esc](#)

[Printer-friendly Version](#)

[Interactive Discussion](#)

Abstract

The cumulative atmospheric nitrogen deposition has been found to profoundly impact the nutrient stoichiometry of the East China seas (ECSs) and the northwestern Pacific Ocean (NWPO). In spite of the potential significance of dry deposition in those regions, ship-board observations of atmospheric aerosols remain insufficient, particularly, for compositions of water-soluble nitrogen species (nitrate, ammonium and water-soluble organic nitrogen – WSON). We conducted a cruise covering the ECSs and the NWPO during the spring of 2014 and observed three types of atmospheric aerosols. AI content, air mass backward trajectory, weather condition, and ion stoichiometry allowed us to discern dust aerosol patches and sea fog modified aerosols (widespread on the ECSs) from background aerosols (open ocean). Among the three types, sea fog modified aerosols contained the highest concentrations of nitrate ($536 \pm 300 \text{ nmol N m}^{-3}$), ammonium ($442 \pm 194 \text{ nmol N m}^{-3}$) and WSON ($147 \pm 171 \text{ nmol N m}^{-3}$); moreover, ammonium and nitrate together occupied $\sim 65\%$ molar fraction of total ions. The dust aerosols also contained significant amounts of nitrate ($100 \pm 23 \text{ nmol N m}^{-3}$) and ammonium ($138 \pm 24 \text{ nmol N m}^{-3}$) which were obviously larger than those in background aerosols (26 ± 32 and $54 \pm 45 \text{ nmol N m}^{-3}$, respectively, for nitrate and ammonium), yet this was not the case for WSON. It appeared that dust aerosols had less of a chance to contact WSON during its transport. In the open ocean, we found that sea salt (e.g. Na^+ , Cl^- , Mg^{2+}), as well as WSON, correlates positively with wind speed. Apparently, marine WSON was emitted during breaking waves. Regardless of the variable wind speeds from 0.8 to as high as 18 m s^{-1} nitrate and ammonium, by contrast, remained in narrow ranges implying that some supply and consumption processes of nitrate and ammonium were required to maintain such a quasi-static condition. Mean dry deposition of total dissolved nitrogen (TDN) for sea fog modified aerosols ($1090 \pm 671 \text{ }\mu\text{mol N m}^{-2} \text{ d}^{-1}$) was 5 times higher than dust aerosols ($190 \pm 41.6 \text{ }\mu\text{mol N m}^{-2} \text{ d}^{-1}$) and around 20 times higher than background aerosols ($56.8 \pm 59.1 \text{ }\mu\text{mol N m}^{-2} \text{ d}^{-1}$). Apparently, spring sea fog on the ECSs played an important role in removing atmospheric reactive nitrogen

Nitrogen speciation in various types of aerosol in spring over the northwestern Pacific Ocean

L. Luo et al.

[Title Page](#)

[Abstract](#)

[Introduction](#)

[Conclusions](#)

[References](#)

[Tables](#)

[Figures](#)

[|◀](#)

[▶|](#)

[◀](#)

[▶](#)

[Back](#)

[Close](#)

[Full Screen / Esc](#)

[Printer-friendly Version](#)

[Interactive Discussion](#)

from the Chinese mainland and depositing it into the ECSs, thus effectively preventing its seaward export to the NWPO.

1 Introduction

Anthropogenic reactive nitrogen (N_r) emissions have dramatically increased in the last 5 decades due to rapidly growing populations and industry (Galloway et al., 2008). China is one of the largest producers and emitters of reactive nitrogen in the world (N_r emission of 12.18 Tgy^{-1} ; Reis et al., 2009). Inevitably, large amounts of reactive nitrogen emanate into its adjacent seas through various pathways. Through the atmosphere, annual nitrogen depositions into the East China seas (ECSs) had been reported to be 10 the same order of magnitude carried by the Yangtze River discharge (Nakamura et al., 2005; Zhang et al., 2007). Besides observational data, global models revealed that both of the Chinese marginal seas and the northwestern Pacific Ocean (NWPO) are under 15 the atmospheric influence of the Asian continent, which supplied significant amounts of anthropogenic reactive nitrogen (Duce et al., 2008) and terrigenous materials (Jickells et al., 2005). The cumulative effect of atmospheric input in the past decades even altered the nutrient stoichiometry on a regional scale, including the Chinese marginal seas and the North Pacific Ocean (T. W. Kim et al., 2011; I. N. Kim et al., 2014).

To better constrain atmospheric deposition of reactive nitrogen to the ocean over 20 large spatial and temporal scales, modeling the transport and deposition of air pollutants is essential. Models of atmospheric nitrogen deposition include abundant parameters, such as local emission densities, particle size, deposition velocity, chemical processes and meteorological conditions (Liu et al., 2005; Guenther et al., 2006; Kanakidou et al., 2012). However, model accuracy strongly relies on the validation by observational data. Unfortunately, ship-board observations, particularly for an offshore 25 gradient from marginal seas to the wide-open sea, are still limited.

Fog and dust storms are two common intermittent weather events in the marginal seas of China during the transition period from a cold to a warm season (Sun et al.,

[Title Page](#)

[Abstract](#)

[Introduction](#)

[Conclusions](#)

[References](#)

[Tables](#)

[Figures](#)

[|◀](#)

[▶|](#)

[◀](#)

[▶](#)

[Back](#)

[Close](#)

[Full Screen / Esc](#)

[Printer-friendly Version](#)

[Interactive Discussion](#)

2001; Zhang et al., 2009). Dust aerosols may serve as a carrier bringing significant amounts of terrigenous and anthropogenic fingerprints including trace elements (Duce et al., 1980) and reactive nitrogen (Chen and Chen, 2008) from inland into the open sea via long-range transport. By contrast, sea fog is relatively stagnant and restricted in spatial scale. Fog chemistry and fog modified aerosols have been studied on land (Yao and Zhang, 2012; Gilardoni et al., 2014) and its impacts on terrestrial ecosystems were also highlighted (Chang et al., 2002; Lange et al., 2003). Compared with inland fog and dust aerosols, we have less knowledge about sea fog chemistry, not to mention the aerosol chemistry under sea fog influence. This is the first investigation 5 of reactive nitrogen speciation and deposition of sea fog modified aerosols (aerosol collected under sea fog influence) on the marginal seas off a continent emitting strong emissions.

Different types of aerosols may be composed of different amounts of nitrogen species according to their formation history (e.g. origin, flow path, reactions during transport). In 15 this study, we sampled total suspended particulate (TSP) marine aerosols on a cruise crossing over the Yellow Sea, East China Sea and northwestern Pacific Ocean during spring 2014. Water-soluble nitrogen species and ion characteristics among different aerosol types, including dust, background and sea fog modified aerosols, were investigated. These observational data promote our understanding about type-specific 20 concentration and deposition of various nitrogen species and the role of sea fog on nitrogen scavenging. The data may aid in validating model outputs for the Asian region and potentially evaluate the framework of nitrogen and aerosol interactions in current models.

Title Page	
Abstract	Introduction
Conclusions	References
Tables	Figures
◀	▶
◀	▶
Back	Close
Full Screen / Esc	
Printer-friendly Version	
Interactive Discussion	

2 Materials and methods

2.1 Aerosol sample collection and chemical analyses

A total of 44 TSP samples were collected by using a high-volume TSP aerosol sampler (TE-5170D; Tisch Environmental Inc.) during a research cruise on the R/V *Dongfanghong II* from 17 March to 22 April 2014. The cruise tracks (Fig. 1) cover the ECSs (Yellow Sea and East China Sea) and the NWPO. The samples were taken at ~ 12 h intervals. To avoid self-contamination from the research vessel, we sampled only when the vessel was cruising; thus, the sampling interval is not exactly 12 h. Detailed sampling information including date, time period and locations for each sample are listed in Table S1. Meteorological data (Fig. 2) including wind speed and direction, relative humidity (RH) and temperature were recorded on-board.

The cruise encountered sea fog in the first few days (orange shadow in Fig. 2 for 17–19 March) and collected five samples (nos. 1–5). Surprisingly, sea fog occurred again on 21–22 April while approaching land (samples nos. 43 and 44). During the fog events, high relative humidity and slow wind speed were recorded (see orange shadow in Fig. 2). The strong temperature gradient indicated that the sea fog formed due to a cold air mass from land confronting warm air from the sea. Since these samples were collected on fog days (see orange tracks in Fig. 1) when we could collect aerosols, the sea fog modified the aerosols as well as sea fog droplets. Since we cannot separate them from each other through our method, we classified these samples as “sea fog modified aerosol”.

Whatman 41 cellulose filters (Whatman Limited, Maidstone, UK) were used for filtration. The analytical procedures were described by Hsu et al. (2010b, 2014). Briefly, one-eighth of the filter was extracted by using 15 mL of Milli-Q water on a reciprocating shaker for 0.5 h and at rest for an additional 0.5 h at room temperature. Then, the extract was filtered through a polycarbonate membrane filter (0.4 µm pore size and 47 mm in diameter from Nuclepore). The filter was leached three times with Milli-Q water, and then 5 mL Milli-Q water was used to rinse the filter. The extract 45 mL solution mixed

[Title Page](#)

[Abstract](#)

[Introduction](#)

[Conclusions](#)

[References](#)

[Tables](#)

[Figures](#)

[|◀](#)

[▶|](#)

[◀](#)

[▶](#)

[Back](#)

[Close](#)

[Full Screen / Esc](#)

[Printer-friendly Version](#)

[Interactive Discussion](#)

with the rinsing 5 mL were poured into a 50 mL clean plastic centrifuge tube and used for the determination of the ion species and water-soluble aluminum (Al).

The water soluble and total concentrations of Al in TSPs were analyzed by inductively coupled plasma mass spectrometers (ICP-MS). For total Al, briefly, one-eighth of the filter was digested with an acid mixture (4 mL HNO_3 + 2 mL HF) using an ultra-high throughput microwave digestion system (MARSXpress, CEM; Corporation, Matthews, NC), and the efficiency of the digestion scheme was checked by subjecting a certain amount of a standard reference material (SRM1648, urban particulate matter, National Institute of Standards and Technology (NIST), USA) to the same treatment. The recoveries of Al in the SRM 1648 through digestion with the HNO_3 -HF mixture fell with $\pm 10\%$ ($n = 5$) of the certified values. Details regarding the ICP-MS analysis were described by Hsu et al. (2008).

Major ionic species (Na^+ , NH_4^+ , K^+ , Mg^{2+} , Ca^{2+} , Cl^- , NO_3^- , NO_2^- and SO_4^{2-}) in the extract were analyzed by ion chromatography (model ICS-1100 for anions and model ICS-900 for cations) equipped with a conductivity detector (ASRS-ULTRA) and suppressor (ASRS-300 for ICS-1100 and CSRS-300 for ICS-900). Separator columns (AS11-HC for anions, and CS12A for cations) and guard columns (AG11-HC for anions, and CG12A for cations) were used in the analyses. The precision for all ionic species were better than 5 %. Detailed analytical processes can be found in Hsu et al. (2014). Only five samples can be detected for NO_2^- (1.39 nmol m^{-3} for no. 2, 2.32 nmol m^{-3} for no. 4, 3.69 nmol m^{-3} for no. 5, 5.96 nmol m^{-3} for no. 43 and 3.76 nmol m^{-3} for no. 44), which account for < 1 % of the TDN.

Total dissolved nitrogen (TDN) were analyzed by the wet oxidation method to convert all nitrogen species into nitrate with re-crystallized potassium persulfate, and then the concentration of nitrate was measured with chemiluminescence (Knapp et al., 2005). Monitoring with laboratory stock ($\text{NO}_3^- + \text{NH}_4^+ + \text{Glycine} + \text{EDTA}$) showed that the recoveries of TDN by the persulfate oxidizing reagent (POR) digestion were falling within 95–105 % ($n = 6$) over the range of detection.

Nitrogen speciation in various types of aerosol in spring over the northwestern Pacific Ocean

L. Luo et al.

[Title Page](#)

[Abstract](#)

[Introduction](#)

[Conclusions](#)

[References](#)

[Tables](#)

[Figures](#)

[|◀](#)

[▶|](#)

[◀](#)

[▶](#)

[Back](#)

[Close](#)

[Full Screen / Esc](#)

[Printer-friendly Version](#)

[Interactive Discussion](#)

2.2 Data analysis

The amount of non-sea-salt Ca^{2+} (nss- Ca^{2+}) and non-sea-salt SO_4^{2-} (nss- SO_4^{2-}) in aerosol, the Ca^{2+} and SO_4^{2-} fractions in excess over that expected from sea salt, were calculated by using the unit of equivalent concentration (neq m^{-3}) in the following equations

$$[\text{nss-}\text{Ca}^{2+}] = [\text{Ca}^{2+}] - [\text{ss-}\text{Ca}^{2+}], \quad \text{where } [\text{ss-}\text{Ca}^{2+}] = 0.044 \times [\text{Na}^+], \quad (1)$$

$$[\text{nss-}\text{SO}_4^{2-}] = [\text{SO}_4^{2-}] - [\text{ss-}\text{SO}_4^{2-}], \quad \text{where } [\text{ss-}\text{SO}_4^{2-}] = 0.121 \times [\text{Na}^+], \quad (2)$$

where the factors of 0.044 and 0.121 used above are the typical calcium-to-sodium and sulfate-to-sodium equivalent molar ratios in seawater.

Relative acidity (RA) was calculated by using all of the observed ion species in their equivalent concentrations following Yao and Zhang (2012):

$$\text{RA} = \frac{[\text{Na}^+] + [\text{Mg}^{2+}] + [\text{K}^+] + [\text{Ca}^{2+}] + [\text{NH}_4^+]}{[\text{Cl}^-] + [\text{NO}_3^-] + [\text{SO}_4^{2-}]}, \quad (3)$$

where $[\text{Na}^+]$, $[\text{Mg}^{2+}]$, $[\text{K}^+]$, $[\text{Ca}^{2+}]$, $[\text{NH}_4^+]$, $[\text{Cl}^-]$, $[\text{NO}_3^-]$ and $[\text{SO}_4^{2-}]$ are the equivalent concentrations of those water extracted ions.

The concentration of water-soluble organic nitrogen (WSON) was calculated with the following equation

$$[\text{WSON}] = [\text{TDN}] - [\text{NO}_3^-] - [\text{NH}_4^+] - [\text{NO}_2^-], \quad (4)$$

where $[\text{TDN}]$, $[\text{NO}_3^-]$, $[\text{NH}_4^+]$ and $[\text{NO}_2^-]$ are molar concentrations (nmol N m^{-3}) of those water-soluble nitrogen species in TSPs. The standard error propagated through WSON calculation was 116 %.

Title Page	
Abstract	Introduction
Conclusions	References
Tables	Figures
◀	▶
◀	▶
Back	Close
Full Screen / Esc	
Printer-friendly Version	
Interactive Discussion	

2.3 Flux calculation

The dry deposition flux (F) was calculated by multiplying the aerosol concentrations of water-soluble nitrogen speciation (C) by the dry deposition velocity (V):

$$F = C \times V, \quad (5)$$

5 where V is a primarily function of particle size and meteorological parameters, such as wind speed, relative humidity and sea surface roughness (Duce et al., 1991). According to previous reports, dry deposition velocity varies by more than 3 orders of magnitude at a particle size ranging from 0.1 to 100 μm (Hoppel et al., 2002), and in our observation wind speed ranging from 0.8 to 18 m s^{-1} under a RH ranging from 10 40 to 100 % (Fig. 2). It is very difficult to provide variable dry deposition velocities under a wide range of environmental conditions (Hoppel et al., 2002); thus, assumptions were made based on existing knowledge. In general, ammonium appears in submicron mode from 0.1 to 1 μm with a small fraction residing in the coarser mode; on the contrary, nitrate is distributed in a supermicron size ranging from 1 to 10 μm (Yao and 15 Zhang, 2012; Hsu et al., 2014). As indicated by Nakamura et al. (2005), both NH_4^+ and NO_3^- exist in both fine and coarse modes; therefore, we keep in mind that a direct use of a fixed deposition rate might cause an under- or overestimation. Unfortunately, we collected TSPs with no information for size distributions. Thus, according to the model and experimental results for aerosols deposition to the sea surface (Duce et al., 1991; 20 Hoppel et al., 2002) and the size distribution of nitrate and ammonium in particles as reported above, deposition velocity of 2 cm s^{-1} was applied for nitrate and 0.1 cm s^{-1} for the ammonium. Both deposition velocities were often used in calculating the specific nitrogen deposition fluxes, especially for the maritime aerosols, though uncertainties were involved (de Leeuw et al., 2003; Nakamura et al., 2005; Chen et al., 2010; Jung et al., 2013). However, size distribution of WSON studies showed that WSON appears 25 in a wide size spectrum (Chen et al., 2010; Lesworth et al., 2010; Srinivas et al., 2011). In previous studies, different orders of magnitude of deposition velocity were employed

Title Page	
Abstract	Introduction
Conclusions	References
Tables	Figures
◀	▶
◀	▶
Back	Close
Full Screen / Esc	
Printer-friendly Version	
Interactive Discussion	

for WSON deposition (1.2 cm s^{-1} by He et al., 2011; 0.1 cm s^{-1} for fine and 1.0 cm s^{-1} for coarse by Srinivas et al., 2011; 0.075 cm s^{-1} for fine and 1.25 cm s^{-1} for coarse by Violaki et al., 2010). Our TSP aerosols cover the entire size distribution; thus, 1.0 cm s^{-1} is applied for WSON deposition. Since 1.0 cm s^{-1} is near the upper boundary of velocities previously applied for WSON deposition, our calculation of WSON deposition may represent the upper boundary.

2.4 Air mass backward trajectory analysis

In order to investigate the likely origins of aerosol in the transporting air masses, 3 days with three heights of above sea level air mass back trajectories were calculated by using the National Oceanic and Atmospheric Administration (NOAA) Hybrid Single Particle Lagrangian Integrated Trajectory (HYSPLIT) model with a $1^\circ \times 1^\circ$ latitude–longitude grid and the final meteorological database. Details about the HYSPLIT model can be found at <https://ready.arl.noaa.gov/HYSPLIT.php>, as prepared by the NOAA Air Resources Laboratory. The time period of 3 days was suggested to be sufficient for dust transport from dust source to the northwestern Pacific Ocean (Husar et al., 2001). The three heights (100, 500, and 1000 m) were selected because 1000 m can be taken as one of the typical atmospheric boundary layers (Hennemuth and Lammert, 2006).

3 Results and discussion

With Al content, air mass backward trajectory, weather condition, and ion stoichiometry, we classify aerosol into three types and then discuss the speciation and concentrations of reactive nitrogen for each aerosol type as well as potential processes involved. We compared chemical characteristics of dust aerosols collected in the ECSs with ours under sea fog influence. Global aerosol and precipitation WSON data were also compiled to reveal the significance of WSON. Finally, we estimated the deposition of individual

Nitrogen speciation in various types of aerosol in spring over the northwestern Pacific Ocean

L. Luo et al.

[Title Page](#)

[Abstract](#)

[Introduction](#)

[Conclusions](#)

[References](#)

[Tables](#)

[Figures](#)

[|◀](#)

[▶|](#)

[◀](#)

[▶](#)

[Back](#)

[Close](#)

[Full Screen / Esc](#)

[Printer-friendly Version](#)

[Interactive Discussion](#)

nitrogen species for three types of aerosol and highlight the importance of atmospheric nitrogen deposition in different regions.

3.1 Aerosol type classification

Total Al content in aerosol samples is an often used index to identify the dust event (Hsu et al., 2008). As shown in Fig. 3, the total Al concentrations in aerosols ranged from 52 to 6293 ng m^{-3} during the entire cruise. For the first three samples (from nos. 1 to 3 collected in the Yellow Sea), total Al increased from 1353 to 6293 ng m^{-3} , and then rapidly decreased (nos. 4 and 5 in East China Sea) as the cruise moved eastward to the NWPO (orange shadow in Fig. 3). When the cruise came back to the ECSs, the total Al concentrations in aerosols (nos. 43 and 44) increased once again. Apparently, an abundance of dust is frequently present in the low atmosphere on the Chinese marginal seas in the spring season. The air mass backward trajectories by HYSPLIT (Fig. 4a) revealed that the air masses for those fog samples mainly hovered over the ECSs at an altitude of $< 500 \text{ m}$ and the air masses for nos. 1–5 originated from the east coast of China. The air masses for the samples of nos. 43–44 were from south of Korea. The water-soluble Al followed the same pattern of total Al (Fig. 3) but the leachable fractions were significantly higher when compared with dust aerosols reported for the same area (see below). The relative acidity of aerosols showed that the values of sea fog modified aerosols were all below 0.9 (Fig. 3) indicating an enhanced acidification relative to those aerosols with sea fog influence. The low RA values explained the higher fractions of water-soluble Al.

As for sample nos. 6, 7, 25–27 and 29 collected in the NWPO (see pink tracks in Fig. 1), the total Al concentrations ranged from 590 to 1480 ng m^{-3} with an average of $1025 \pm 316 \text{ ng m}^{-3}$ (pink shadow in Fig. 3), which were significantly higher than the remaining samples ($212 \pm 120 \text{ ng m}^{-3}$) from the NWPO. Although most the air mass backward trajectories of those samples collected in the NWPO originated from 25° N to 40° N (and beyond) as well as high altitude (Fig. 4b), the lidar browse images from NASA (Fig. S1) clearly indicate that the air mass of those aerosol samples pass

Title Page	
Abstract	Introduction
Conclusions	References
Tables	Figures
◀	▶
◀	▶
Back	Close
Full Screen / Esc	
Printer-friendly Version	
Interactive Discussion	

through dusty regions. Based on distinctive total Al concentrations and air mass pathway, we separated dust aerosols from the background aerosols collected in the NWPO.

Below we can also see discernable ion stoichiometry among three types.

3.2 Ion stoichiometry in three types of aerosol

Excluding sea fog modified aerosols, all the ratios of total anions and total cations followed close to a 1 : 1 liner relation (Fig. 5a). Such a well-defined positive relation indicated the charge balance and further emphasized the validity of our measurements. The sea fog modified aerosols in the ECSs contained higher contents of anions than cations, which was consistent with previous observation for fog water (Chang et al., 2002; Lange et al., 2003; Yue et al., 2014). Non-measured H^+ ion, should be the dominant cation for charge compensation as indicated previously (Chang et al., 2002; Lange et al., 2003). The low RA values for sea fog modified aerosols also support this notion (Fig. 3). Below we illustrated characteristics of three types of aerosols with ion stoichiometry.

Since the Cl^-/Na^+ ratios of all samples including sea fog modified aerosols (Fig. 5b) were near 1.17, indicated that almost all the Na and Cl for our aerosols originated from sea salt. The relation between Mg^{2+} vs. Na^+ (Fig. 5c) illustrated that almost all Mg^{2+} originated from sea salt sources ($\text{Mg}/\text{Na}_{\text{ss}} = 0.23$) except sea fog modified aerosols, which held a deviated correlation due to Mg enrichment ($y = 0.32x + 8.7$, $R^2 = 0.88$) because of terrestrial mineral sources of Mg. Such Mg enrichment had not been observed in summer sea fog in the subarctic North Pacific Ocean (Jung et al., 2013).

As for Ca^{2+} (Fig. 5d), all types of aerosol were enriched in Ca^{2+} but at different levels, indicating various degrees of terrestrial mineral influence on the marine aerosols. For background aerosols, a strong correlation between Ca^{2+} and Na^+ ($y = 0.044x + 6.6$, $R^2 = 0.92$) was observed. The slope is identical to that of sea water ($\text{Ca}/\text{Na}_{\text{ss}} = 0.044$) suggesting that most Ca^{2+} and Na^+ in background aerosols were sourced from sea salt. An unusually high regression slope ($20 \times$ the sea salt) observed between Ca^{2+}

[Title Page](#)

[Abstract](#)

[Introduction](#)

[Conclusions](#)

[References](#)

[Tables](#)

[Figures](#)

[|◀](#)

[▶|](#)

[◀](#)

[▶](#)

[Back](#)

[Close](#)

[Full Screen / Esc](#)

[Printer-friendly Version](#)

[Interactive Discussion](#)

and Na^+ in sea fog modified aerosols ($y = 0.90x - 1.8$, $R^2 = 0.71$) was attributable to the reaction between mineral CaCO_3 and H^+ in fog droplets during the formation of sea fog (Yue et al., 2012). More excessive Ca^{2+} observed in dust aerosols implied stronger heterogeneous reactions between the acid gas and dust minerals had occurred during long-range transport (Hsu et al., 2014). Similar to Ca^{2+} , patterns between K^+ and Na^+ can also be seen in Fig. 5e. However, besides the contribution from inland dust (Savoie and Prospero, 1980) excess K^+ may also originate from the biomass burning in China (Hsu et al., 2009). Note that statistically significant intercepts can be seen in Ca^{2+} against Na_{ss} and K^+ against Na_{ss} scatter plots for background aerosols. Though small, such excesses in Ca^{2+} and K^+ relative to Na^+ in widespread background aerosols warrant explanations. It might be associated with fertilized soil that contains Ca^{2+} and K^+ ; alternatively, it could be attributed to the spatial heterogeneity of these ions in sea water. No substantial evidence can support both speculations leaving the cause for the trivial intercepts unanswered.

As shown in Fig. 5f, a correlation was found between NH_4^+ and nss-SO_4^{2-} . Except for three sea fog samples, all ratios fall close to the 1 : 1 regression line suggesting the dominance of $(\text{NH}_4)_2\text{SO}_4$ rather than NH_4HSO_4 . Complete neutralization of NH_4^+ by nss-SO_4^{2-} had likely occurred, and a similar phenomenon was found elsewhere (Zhang et al., 2013; Hsu et al., 2014).

The ratio of $[\text{NO}_3^- + \text{nss-SO}_4^{2-}] / [\text{NH}_4^+ + \text{nss-Ca}^{2+}]$ for background aerosols (Fig. 5g) closely follows the unity that suggests that $\text{NH}_4^+ + \text{nss-Ca}^{2+}$ was neutralized by the acidic ions NO_3^- and nss-SO_4^{2-} . However, for the dust and foggy aerosols, $[\text{NO}_3^- + \text{nss-SO}_4^{2-}] / [\text{NH}_4^+ + \text{nss-Ca}^{2+}]$ ratios located between 1 : 1 and 2 : 1 indicate that excessive anthropogenic acidic ions that originated from coal fossil fuel combustion and vehicle exhaust had been transported to the ECSs and NWPO by Asian winter monsoon as indicated previously (Hsu et al., 2010a). As shown in Fig. 5h, the scatter plot of NH_4^+ against NO_3^- revealed that almost all dust and background aerosols sampled in the NWPO have $\text{NH}_4^+ / \text{NO}_3^-$ ratios larger than 1, which is common in aerosol observa-

Nitrogen speciation in various types of aerosol in spring over the northwestern Pacific Ocean

L. Luo et al.

Title Page

Abstract

Introduction

Conclusions

References

Tables

Figures

|◀

▶|

◀

▶

Back

Close

Full Screen / Esc

Printer-friendly Version

Interactive Discussion

tion. However, significantly enriched NO_3^- in sea fog modified aerosols drew the ratio down to < 1 . Nevertheless, such relatively enriched nitrate to ammonium was consistent with a previous study of sea fog water collected from the South China Sea (Yue et al., 2012). In summary, the three types of aerosol have distinctive features in nitrogen speciation and ion stoichiometry including relative acidity (Fig. 6a) further support our aerosol type classification.

3.3 Nitrogen speciation and associated processes in different types of aerosol

3.3.1 Sea fog modified aerosols

There were only a few studies about water-soluble nitrogen species reported in sea fog water (Sasakawa and Uematsu, 2002; Yue et al., 2012; Jung et al., 2013). To the best of our knowledge, this is the first first-hand data from the Chinese marginal seas (Yellow Sea and East China Sea) in spring about water-soluble nitrogen species in aerosol collected under the influence of sea fog. As shown in Table 1 and Fig. 6a, in sea fog modified aerosols the concentrations of nitrate ranged from 160 to $1118 \text{ nmol N m}^{-3}$ with a mean of $536 \pm 300 \text{ nmol N m}^{-3}$ and ammonium was slightly lower than nitrate ranging from 228 to $777 \text{ nmol N m}^{-3}$ with a mean of $442 \pm 194 \text{ nmol N m}^{-3}$. WSON in sea fog modified aerosols was the lowest nitrogen species ranging from 23 to $517 \text{ nmol N m}^{-3}$ with a mean of $147 \pm 171 \text{ nmol N m}^{-3}$ (Table 1 and Fig. 6a). The sea fog modified aerosols contained 2–11 times higher concentration in nitrate, 2–6 times higher ammonium and 3–6 times higher WSON when compared with aerosols in the ECSs and other regions (Table 1). Such high concentrations of reactive nitrogen not only highlights the seriousness of the nitrogen air pollution in Chinese marginal seas, but also underscores that water-soluble nitrogen species can be scavenged efficiently during sea fog formation.

The seven sea fog modified aerosols were also distinctive in chemical characteristics when compared specifically with the dust aerosols from the same region. The concentrations of leachable ions, water-soluble and total AI and RA for dust aerosols and sea

L. Luo et al.

[Title Page](#)

[Abstract](#)

[Introduction](#)

[Conclusions](#)

[References](#)

[Tables](#)

[Figures](#)

[|◀](#)

[▶|](#)

[◀](#)

[▶](#)

[Back](#)

[Close](#)

[Full Screen / Esc](#)

[Printer-friendly Version](#)

[Interactive Discussion](#)

fog modified aerosols sampled in the ECSs are listed in Table 2 for comparison. For all except NH_4^+ , NO_3^- and SO_4^{2-} , sea fog modified aerosols have lower or similar molar concentrations relative to dust aerosols. The anthropogenic species, particularly NO_3^- and NH_4^+ , were the most abundant ions in the sea fog modified aerosols. On the contrary, Na^+ and Cl^- were the highest among all the ions in dust aerosols from the island of Jeju and the East China Sea. Taking Jeju as example, the concentration levels of Na^+ and Cl^- were similar to that of our sea fog modified aerosols, yet both NO_3^- and NH_4^+ in sea fog modified aerosols were > 6 times higher than those from the island of Jeju.

In a previous study in Po Valley, the average scavenging efficiency for aerosol nitrate and ammonium were reported to be at similar levels (70 and 68 %, respectively) (Gillardoni et al., 2014), while in our case the concentrations of nitrate in sea fog modified aerosols were higher than those of ammonium (Table 1 and Fig. 6a). Since the gas phase HNO_3 is rapidly dissolved in liquid water particles during the early stages of fog formation (Fahey et al., 2005; Moore et al., 2004), it is reasonable to infer enriched nitrate in sea fog was attributed to gaseous HNO_3 due to the gas–liquid equilibrium between NO_3^- and HNO_3 in fog droplet. Moreover, our sea fog modified aerosols were collected from the air masses roaming around east China and the ECSs, where the NO_x emission is the highest in China (Gu et al., 2012). Accordingly, nitrate enrichment on sea fog modified aerosol was likely a synergistic consequence due to the sea fog formation and gas–liquid equilibrium of gaseous HNO_3 .

The pie charts of ion fractions of aerosols from the ECSs were shown in Fig. 7. Note that the fraction distribution of ions for the dust aerosols from a previous cruise in the ECS ($n = 8$, Fig. 7b) resembled that collected from the island of Jeju ($n = 49$, Fig. 7c) despite their sampling differences in space and time. Such consistency in the ion pie chart indicated the representativeness of these dust aerosols. However, the pie chart for sea fog modified aerosols revealed that NH_4^+ and NO_3^- occupied approximately 30 and 36 %, respectively, of the total ionic concentration (Fig. 7a). Such overwhelmingly

L. Luo et al.

[Title Page](#)

[Abstract](#)

[Introduction](#)

[Conclusions](#)

[References](#)

[Tables](#)

[Figures](#)

[|◀](#)

[▶|](#)

[◀](#)

[▶](#)

[Back](#)

[Close](#)

[Full Screen / Esc](#)

[Printer-friendly Version](#)

[Interactive Discussion](#)

high occupation of nitrogenous ions emphasized the role of sea fog in modifying the chemistry of non-foggy dust aerosols.

As for SO_4^{2-} , both the concentration and percent occupation were comparable in sea fog modified aerosols and dust aerosols (Table 2 and Fig. 7). However, the concentrations of nss- SO_4^{2-} in sea fog modified aerosols was 60 % higher than those of dust aerosols (Table 2), suggesting the addition of anthropogenic SO_x emissions during sea fog formation as indicated by Gilardoni et al. (2014). In the marginal seas adjacent to the anthropogenic emission source, acidified sea fog induced by additional sulfuric and nitric acid was common (Sasakawa and Uematsu, 2005; Yue et al., 2014); however, as mentioned in Fig. 5f, nearly all the nss- SO_4^{2-} was neutralized by NH_4^+ in sea fog modified aerosols; thus, the acidity was caused mainly by the excessive NO_3^- .

In general, Al in marine aerosols originated from terrestrial minerals (Uematsu et al., 2010). The mean concentrations of total Al in these seven sea fog samples were the lowest among those in dust aerosols from the ECSs (Table 2). However, the concentrations of water-soluble Al in sea fog modified aerosols were significantly higher than those of dust aerosols. Due to the high acidity (low RA values) for sea fog modified aerosols (Fig. 6a), we suspected that during the seasonal transition period the formation of sea fog at the land–ocean boundary may acidify the aerosol to promote the solubility of metals in aerosol mineral effectively.

Finally, it had been shown that dissolved organic matter can be scavenged by fog, but its scavenging efficiency was lower than those of nitrate and ammonium due to hydrophobic organic species more difficult to be scavenged than hydrophilic (Maria and Russell, 2005; Gilardoni et al., 2014). In our case, although concentrations of WSON in sea fog modified aerosols ($147 \pm 171 \text{ nmol N m}^{-3}$) were significantly higher than those of background aerosols, the ratio of WSON to TDN in sea fog modified aerosols ($10 \pm 6 \%$) was similar to those of (range from 10 to 24 %) background aerosols sampled in the ECSs (Table 1). Low fraction of WSON in TDN may indicate, but not necessarily, the low scavenging efficiency of WSON. More studies are needed to probe the role of WSON during sea fog formation.

Nitrogen speciation in various types of aerosol in spring over the northwestern Pacific Ocean

L. Luo et al.

[Title Page](#)

[Abstract](#)

[Introduction](#)

[Conclusions](#)

[References](#)

[Tables](#)

[Figures](#)

[I◀](#)

[▶I](#)

[◀](#)

[▶](#)

[Back](#)

[Close](#)

[Full Screen / Esc](#)

[Printer-friendly Version](#)

[Interactive Discussion](#)

3.3.2 Dust aerosols

For dust aerosols collected in the NWPO, nitrate ranged from 79 to 145 nmol N m⁻³ with an average of 100 ± 23 nmol N m⁻³ and ammonium ranged from 94 to 163 nmol N m⁻³ with an average of 138 ± 24 nmol N m⁻³ (Table 1 and Fig. 6a). Relative to background aerosols, both nitrate and ammonium were significantly higher in dust aerosols revealing the anthropogenic nitrogen fingerprint carried by the Asian dust outflow along with westerlies (Chen and Chen, 2008). Interestingly, dust aerosols contained a low concentration of WSON (11.2 ± 4.0 nmol N m⁻³) resembling that of background aerosols (Table 1 and Fig. 6a). Moreover, dust aerosols held the lowest WSON fraction in total dissolved nitrogen among three types (Table 1 and Fig. 6b). Based on a good correlation between nss-Ca²⁺ and WSON, previous studies demonstrated that dust can carry anthropogenic “nitrogen” activity into remote oceans and simultaneously promote the ratio of WSON / TDN in aerosol (Mace et al., 2003b; Lesworth et al., 2010; Violaki et al., 2010). However, in our case there was no correlation between WSON and nss-Ca²⁺ (not shown) likely illustrating that these aerosols had less chance to contact WSON along their pathway from a high altitude or WSON had been scavenged during transport. But the latter one was less likely.

3.3.3 Background aerosols

For the 31 background aerosol samples, the mean concentrations of NO₃⁻ and NH₄⁺ were 26 ± 32 and 54 ± 45 nmol N m⁻³, respectively (Table 1). Both were 10 times higher than those collected in the same region during summer (2.5 ± 1.0 nmol N m⁻³ for nitrate and 5.9 ± 2.9 nmol N m⁻³ for ammonium, Jung et al., 2011). The 10 times higher reactive nitrogen for springtime background aerosols indicated that “spring background” is not pristine at all. Such distinctive seasonality was ascribed to origins of air mass since in summer the air masses in our study area were mainly from the open ocean while in spring the air masses were coming from the northeast of China through the Japanese Sea and Japan (Fig. 4c), where they were strongly influenced by anthropogenic nitro-

Title Page	
Abstract	Introduction
Conclusions	References
Tables	Figures
◀	▶
◀	▶
Back	Close
Full Screen / Esc	
Printer-friendly Version	
Interactive Discussion	

gen emission (Kang et al., 2010). The concentration of WSON in background aerosols was $10.9 \pm 6.8 \text{ nmol N m}^{-3}$, which fell within the wide range reported previously (~ 1 to 76 nmol N m^{-3} ; Table 1). In the open ocean, the WSON in aerosol may come from natural and anthropogenic sources. In our background aerosols, insignificant correlation between WSON and nss- Ca^{2+} (not shown) excluded the anthropogenic influence on WSON. Alternatively, biogenic activity in the ocean can be a primary WSON source for atmosphere. For example, the highest percent of WSON in TDN for the case in southern Atlantic (84 %) was attributed to high biological productivity (Violaki et al., 2015). Unfortunately, no substantial evidence was found in our case to support natural WSON source from marine.

Nevertheless, our sampling cruise experienced a wide range of wind speed with variable sea salt contents during collection of background aerosols. The correlations between ion content and wind speed may reveal some useful information. Higher sea salt, e.g. Na^+ , Cl^- , Mg^{2+} , appeared with higher wind speed conditions (Fig. 8a–c). Positive correlations can be seen although r square values were small possibly due to time-integrated sampling ($\sim 12 \text{ h}$) and averaged wind speed over sampling period. The positive correlation illustrated that the emission of sea salt aerosols was driven by wind intensity as indicated by Shi et al. (2012). Except for WSON (Fig. 8d), which was consistent with sea salt associated ions, no statistically significant relations can be derived from scatter plots of nitrate and ammonium against wind speed (Fig. 8e and f). Analogous tendency between WSON and sea salt ions suggested that WSON might come from the surface ocean. Since concentration of WSON in surface sea water was less variable ranging from 4.5 to $5.0 \mu\text{M}$ in the Pacific Ocean (Knapp et al., 2011), WSON can be taken as a relatively constant component in surface sea water similar to Na^+ , Cl^- and Mg^{2+} . Very likely, breaking waves and sea spray brought WSON into the atmosphere under higher wind speed. In fact, by using free amino acids and urea compositions in maritime aerosols Mace et al. (2003a) indicated that live species in the sea surface microlayer may serve as a source of atmospheric organic nitrogen.

L. Luo et al.

[Title Page](#)[Abstract](#)[Introduction](#)[Conclusions](#)[References](#)[Tables](#)[Figures](#)[|◀](#)[▶|](#)[◀](#)[▶](#)[Back](#)[Close](#)[Full Screen / Esc](#)[Printer-friendly Version](#)[Interactive Discussion](#)

In contrast to WSON, nitrate and ammonium presented narrow concentration ranges (except a few highs collected near Japan). Since the concentrations of nitrate and ammonium in the surface ocean were too low (a few tens to hundreds of nM) to sustain the invariable nitrate and ammonium in background aerosols under various sea salt emission conditions, we suggested that removal and supply of nitrate and ammonium in low atmosphere above the ocean surface were likely quasi-static and maintained by some processes such as deposition from upper atmosphere and photochemical production/consumption.

5 Base on $\delta^{15}\text{N}-\text{NH}_4^+$ in aerosol (Jickells et al., 2003) and rainwater (Altieri et al., 2014) collected in Atlantic, ocean was suggested to be one of the ammonium sources for the atmosphere. According to the low concentration of ammonium in the ocean surface, direct ammonium emission via sea spray was less likely. Based on our observation, we hypothesized that emitted marine WSON in the atmosphere may serve as a precursor for ammonium and/or nitrate via photo-degradation and photo-oxidation processes reported previously (Spokes and Liss, 1996; Vione et al., 2005; Xie et al., 2012). More 10 studies about the exchange processes among nitrogen species through the ocean–atmosphere boundary layer are needed.

3.4 WSON in aerosol and rainwater: a global comparison

Organic nitrogen, distributed in gas, particulate and dissolved phases, is an important 20 component in the atmospheric nitrogen cycle. In our case, mean fractions of WSON in aerosol TDN were 10 ± 6 , 5 ± 2 , and 14 ± 8 %, respectively, for modified sea fog, dust and background aerosols. All values fell within the wide range reported previously (also in Table 1). Here we synthesized a published data set about aerosol WSON from 25 around the world for comparison (Fig. 9a). The synthesized data revealed that aerosol WSON concentrations varied over 3 orders of magnitude and the fraction of WSON in TDN ranged from 1 % to as high as 85 %. Additionally, the fraction of WSON is the less variable toward high WSON concentrations. The slope of the liner regression between WSON and TDN indicates that WSON accounts for 18 % of aerosol TDN.

[Title Page](#)

[Abstract](#)

[Introduction](#)

[Conclusions](#)

[References](#)

[Tables](#)

[Figures](#)

[|◀](#)

[▶|](#)

[◀](#)

[▶](#)

[Back](#)

[Close](#)

[Full Screen / Esc](#)

[Printer-friendly Version](#)

[Interactive Discussion](#)

In Fig. 9b, we made a comparison between the distribution of WSON fraction in rainwater TDN (data from Cornell, 2011; Altieri et al., 2012; Zhang et al., 2012; Cui et al., 2014; Chen et al., 2015; Yan and Kim, 2015) and that in aerosol (Mace et al., 2003a; Chen et al., 2007; Lesworth et al., 2010; Shi et al., 2010; Miyazaki et al., 2011; Srinivas et al., 2011; Zamora et al., 2011; Violaki et al., 2015). The distribution pattern of WSON fractions in aerosols (Fig. 9b, grey bar) was relatively concentrated revealing a tendency toward lower fractions. Its peak frequency appeared at the category of 10–20 % and at least 80 % of the observed WSON fractions fell within the range of < 25 %. However, for WSON/TDN in rainwater (Fig. 9b, blue bar), the distribution pattern was relatively diffusive shifting toward a higher percentage and peaking at around categories of 25–40 % with a mean value of 33 % ($n = 332$), which is slightly higher than that (24 %, $n = 115$) obtained by Jickells et al. (2013). Although values of the coefficient of variation for both aerosol and rainwater were high, the results are still statistically meaningful. The mean WSON fraction for rainwater was around 2 times that for aerosol (18 %). In a previous study, Mace et al. (2003a) reported that the fractional contribution of dissolved free amino acids to organic nitrogen in rainwater was 4 times higher than that in aerosol. The higher fractional contribution of WSON to TDN for rainwater may imply that precipitation washed out hydrophilic organic matter or WSON from the atmosphere more effectively (Maria and Russell, 2005).

3.5 Dry deposition of TDN and implications

As shown in Fig. 10, the atmospheric nitrogen dry deposition over the cruise revealed a large spatial variance under different weather conditions. In the ECSs, the mean DIN ($\text{NH}_4^+ + \text{NO}_3^-$) deposition on fog days was estimated to be $\sim 960 \mu\text{mol N m}^{-2} \text{d}^{-1}$ (926 ± 518 and $38 \pm 17 \mu\text{mol N m}^{-2} \text{d}^{-1}$, respectively, for nitrate and ammonium), which was around 6 times higher than the average values for ordinary aerosol derived from literature reports ($153 \mu\text{mol N m}^{-2} \text{d}^{-1}$ for aerosol nitrate and $12.3 \mu\text{mol N m}^{-2} \text{d}^{-1}$ for aerosol ammonium; see Table 3). The WSON deposition ranged from 20 to

Title Page	
Abstract	Introduction
Conclusions	References
Tables	Figures
◀	▶
◀	▶
Back	Close
Full Screen / Esc	
Printer-friendly Version	
Interactive Discussion	

446 $\mu\text{mol N m}^{-2} \text{d}^{-1}$ with an average of $127 \pm 148 \mu\text{mol N m}^{-2} \text{d}^{-1}$. Since the bioavailability of aerosol WSON to phytoplankton was reported to be high (12–80%; Bronk et al., 2007; Wedyan et al., 2007) by adding WSON into the consideration, the deposition of TDN will be $\sim 1100 \mu\text{mol N m}^{-2} \text{d}^{-1}$.

By taking $1150 \times 10^3 \text{ km}^2$ for the total area cover by the ECSs (Yellow sea and East China Sea) we calculated the daily nitrogen supply from atmospheric deposition associated with sea fog to be $18 \pm 11 \text{ Gg TDN d}^{-1}$, which is around 6 times the nitrogen input from the Yangtze River in spring (total amount of $3.1 \text{ Gg DIN d}^{-1}$; Li et al., 2011) and 2 times the supply from subsurface intrusion of Kuroshio ($7.9 \text{ Gg NO}_3^- \text{-N d}^{-1}$; Chen, 1996). In the ECSs, the sea fog occurrence is reported to be around 3–5 days in March and 8–10 days in April (Zhang et al., 2009). Given such high TDN deposition per day, the contribution of foggy weather should really be taken into account on a monthly estimate even though the occurrence of sea fog is limited in time and space. Moreover, the atmospheric influence is more widespread than the river focusing on the plume area.

By assuming that nitrogen is the limiting nutrient and all the total dissolved nitrogen deposited from atmosphere into the sea is bioavailable and will be utilized for carbon fixation, we obtained a C-fixation rate of $\sim 87 \text{ mg C m}^{-2} \text{ d}^{-1}$ in spring for the ECSs based on the Redfield C/N ratio of 6.6. Since the atmospheric nitrogen deposition is an external source, such a conversion represents new production. When compared with the primary productivity in the East China Sea ($292\text{--}549 \text{ mg C m}^{-2} \text{ d}^{-1}$; Gong et al., 2000), the new production associated with sea fog nitrogen deposition may account for 16–30 % of the primary production in the ECSs on foggy days in spring.

Similar to sea fog on the ECSs, sporadic dust events are frequently observed from March to May in the NWPO (Shao and Dong, 2006). In our spring case, the average deposition of dust aerosol nitrate and ammonium ($172 \pm 40 \mu\text{mol N m}^{-2} \text{ d}^{-1}$ for nitrate and $11.9 \pm 2.1 \mu\text{mol N m}^{-2} \text{ d}^{-1}$ for ammonium) were significantly higher than that of background aerosols ($44.6 \pm 55.3 \mu\text{mol N m}^{-2} \text{ d}^{-1}$ for nitrate and $4.7 \pm 4.0 \mu\text{mol N m}^{-2} \text{ d}^{-1}$ for ammonium; see Table 3). However, both dust and background aerosols depositions were significantly higher in spring when compared to summer time dry deposition in

Title Page

Abstract

Introduction

Conclusions

References

Tables

Figures

|◀

▶|

◀

▶|

Back

Close

Full Screen / Esc

Printer-friendly Version

Interactive Discussion

the subtropical western North Pacific (3.0 ± 1.5 and $2.7 \pm 2.1 \mu\text{mol N m}^{-2} \text{d}^{-1}$, respectively, for nitrate and ammonium) and the subarctic western North Pacific (3.3 ± 2.3 and $1.9 \pm 0.63 \mu\text{mol N m}^{-2} \text{d}^{-1}$, respectively, for nitrate and ammonium) (Jung et al., 2011). Likewise, the C-fixation rate in the NWPO during spring was thus estimated to be $4.5\text{--}15 \text{ mg C m}^{-2} \text{ d}^{-1}$ based on the aforementioned assumption and observations. The minimally level of C-fixation induced by dry deposition, in fact, equals to the maximum carbon uptake ($3.6 \text{ mg C m}^{-2} \text{ d}^{-1}$; Jung et al., 2013) in summer by the total atmospheric DIN deposition (wet + dry + sea fog) in the western North Pacific Ocean. Thus, the contribution of atmospheric nitrogen deposition in spring to primary production in the NWPO could be significant between seasons.

4 Conclusions

1. This is first-hand data of total dissolved nitrogen species in TSPs over the ECSs collected under spring sea fog influence. Base on multiple criteria, we successfully classified samples into three types: sea fog modified aerosols, dust and background aerosols.
2. Among the three types, sea fog modified aerosols contain the highest concentrations for all nitrogen species with higher acidity and cation deficiency.
3. Compared to background aerosols, the dust aerosols were significantly enriched in nitrate and ammonium, but not in WSON. Unless WSON-depletion processes had occurred, such disproportionate enrichment suggested that dust aerosols from high latitude and altitude may have less of a chance to contact WSON during the long-range transport.
4. In the open sea, WSON revealed a pattern similar to sea salt ions (Na^+ , Mg^{2+} and Cl^-) whereby concentrations increased as the wind speed increased. Such resemblance indicated that WSON might come from the surface ocean sharing

Nitrogen speciation in various types of aerosol in spring over the northwestern Pacific Ocean

L. Luo et al.

[Title Page](#)

[Abstract](#)

[Introduction](#)

[Conclusions](#)

[References](#)

[Tables](#)

[Figures](#)

[|◀](#)

[▶|](#)

[◀](#)

[▶](#)

[Back](#)

[Close](#)

[Full Screen / Esc](#)

[Printer-friendly Version](#)

[Interactive Discussion](#)



the same emission processes as sea salt. In contrast, ammonium and nitrate concentrations revealed no correlation with the content of sea salt (scavenger). It is likely that nitrate and ammonium in the sea surface atmosphere had reached a budget balance.

5 5. Distinctive nitrogen deposition fluxes on the spatial scale were governed primarily by weather condition and air mass source.

10 6. Sea fog formation significantly altered the aerosol chemistry. Sea fog associated deposition and chemical processes require more attention and need to be considered in future aerosol monitoring especially in the marginal sea during the seasonal transition.

**The Supplement related to this article is available online at
doi:10.5194/acpd-15-25583-2015-supplement.**

15 *Acknowledgements.* This research was funded by the Major State Basic Research Development Program of China (973 program) (nos. 2014CB953702 and 2015 CB954003), National Natural Science Foundation of China (NSFC U1305233, 91328207 and 41121091). We also thank Peirang Yu and Tianfeng Guo (Ocean University of China) for helping us to collect samples during the cruise and Shuen-Hsin Lin (Academia Sinica in Taiwan) for chemical analyses.

References

20 Altieri, K. E., Hastings, M. G., Peters, A. J., and Sigman, D. M.: Molecular characterization of water soluble organic nitrogen in marine rainwater by ultra-high resolution electrospray ionization mass spectrometry, *Atmos. Chem. Phys.*, 12, 3557–3571, doi:10.5194/acp-12-3557-2012, 2012.

Altieri, K., Hastings, M., Peters, A., Oleynik, S., and Sigman, D.: Isotopic evidence for a marine ammonium source in rainwater at Bermuda, *Global Biogeochem. Cy.*, 28, 1066–1080, 2014.

Title Page	
Abstract	Introduction
Conclusions	References
Tables	Figures
◀	▶
◀	▶
Back	Close
Full Screen / Esc	
Printer-friendly Version	
Interactive Discussion	

Nitrogen speciation in various types of aerosol in spring over the northwestern Pacific Ocean

L. Luo et al.

Bronk, D. A., See, J. H., Bradley, P., and Killberg, L.: DON as a source of bioavailable nitrogen for phytoplankton, *Biogeosciences*, 4, 283–296, doi:10.5194/bg-4-283-2007, 2007.

Chang, S.-C., Lai, I.-L., and Wu, J.-T.: Estimation of fog deposition on epiphytic bryophytes in a subtropical montane forest ecosystem in northeastern Taiwan, *Atmos. Res.*, 64, 159–167, 2002.

Chen, C.: The Kuroshio intermediate water is the major source of nutrients on the East China Sea continental shelf, *Oceanol. Acta*, 19, 523–527, 1996.

Chen, H.-Y. and Chen, L.-D.: Importance of anthropogenic inputs and continental-derived dust for the distribution and flux of water-soluble nitrogen and phosphorus species in aerosol within the atmosphere over the East China Sea, *J. Geophys. Res.*, 113, D11303, doi:10.1029/2007jd009491, 2008.

Chen, H. Y., Chen, L. D., Chiang, Z. Y., Hung, C. C., Lin, F. J., Chou, W. C., Gong, G. C., and Wen, L. S.: Size fractionation and molecular composition of water-soluble inorganic and organic nitrogen in aerosols of a coastal environment, *J. Geophys. Res.-Atmos.*, 115, D22307, doi:10.1029/2010JD014157, 2010.

Chen, Y., Mills, S., Street, J., Golan, D., Post, A., Jacobson, M., and Paytan, A.: Estimates of atmospheric dry deposition and associated input of nutrients to Gulf of Aqaba seawater, *J. Geophys. Res.-Atmos.*, 112, D04309, doi:10.1029/2006JD007858, 2007.

Chen, Y.-X., Chen, H.-Y., Wang, W., Yeh, J.-X., Chou, W.-C., Gong, G.-C., Tsai, F.-J., Huang, S.-J., and Lin, C.-T.: Dissolved organic nitrogen in wet deposition in a coastal city (Keelung) of the southern East China Sea: origin, molecular composition and flux, *Atmos. Environ.*, 112, 20–31, 2015.

Cornell, S. E.: Atmospheric nitrogen deposition: revisiting the question of the importance of the organic component, *Environ. Pollut.*, 159, 2214–2222, 2011.

Cui, J., Zhou, J., Peng, Y., He, Y. Q., Yang, H., Xu, L. J., and Chan, A.: Long-term atmospheric wet deposition of dissolved organic nitrogen in a typical red-soil agro-ecosystem, Southeastern China, *Environ. Sci. Processes Impacts*, 16, 1050–1058, 2014.

de Leeuw, G., Spokes, L., Jickells, T., Skjøth, C. A., Hertel, O., Vignati, E., Tamm, S., Schulz, M., Sørensen, L.-L., and Pedersen, B.: Atmospheric nitrogen inputs into the North Sea: effect on productivity, *Cont. Shelf Res.*, 23, 1743–1755, 2003.

Duce, R., Unni, C., Ray, B., Prospero, J., and Merrill, J.: Long-range atmospheric transport of soil dust from Asia to the tropical North Pacific: temporal variability, *Science*, 209, 1522–1524, 1980.

[Title Page](#)

[Abstract](#)

[Introduction](#)

[Conclusions](#)

[References](#)

[Tables](#)

[Figures](#)

[|◀](#)

[▶|](#)

[◀](#)

[▶](#)

[Back](#)

[Close](#)

[Full Screen / Esc](#)

[Printer-friendly Version](#)

[Interactive Discussion](#)

**Nitrogen speciation
in various types of
aerosol in spring over
the northwestern
Pacific Ocean**

L. Luo et al.

Duce, R., Liss, P., Merrill, J., Atlas, E., Buat-Menard, P., Hicks, B., Miller, J., Prospero, J., Ari-moto, R., and Church, T.: The atmospheric input of trace species to the world ocean, *Global Biogeochem. Cy.*, 5, 193–259, 1991.

Duce, R., LaRoche, J., Altieri, K., Arrigo, K., Baker, A., Capone, D., Cornell, S., Dentener, F., Galloway, J., and Ganeshram, R.: Impacts of atmospheric anthropogenic nitrogen on the open ocean, *Science*, 320, 893–897, 2008.

Fahey, K., Pandis, S., Collett, J., and Herckes, P.: The influence of size-dependent droplet composition on pollutant processing by fogs, *Atmos. Environ.*, 39, 4561–4574, 2005.

Galloway, J. N., Townsend, A. R., Erisman, J. W., Bekunda, M., Cai, Z., Freney, J. R., Martinelli, L. A., Seitzinger, S. P., and Sutton, M. A.: Transformation of the nitrogen cycle: recent trends, questions, and potential solutions, *Science*, 320, 889–892, 2008.

Gilardoni, S., Massoli, P., Giulianelli, L., Rinaldi, M., Paglione, M., Pollini, F., Lanconelli, C., Poluzzi, V., Carbone, S., Hillamo, R., Russell, L. M., Faccini, M. C., and Fuzzi, S.: Fog scavenging of organic and inorganic aerosol in the Po Valley, *Atmos. Chem. Phys.*, 14, 6967–6981, doi:10.5194/acp-14-6967-2014, 2014.

Gong, G.-C., Shiah, F.-K., Liu, K.-K., Wen, Y.-H., and Liang, M.-H.: Spatial and temporal variation of chlorophyll a, primary productivity and chemical hydrography in the southern East China Sea, *Cont. Shelf Res.*, 20, 411–436, 2000.

Gu, B., Ge, Y., Ren, Y., Xu, B., Luo, W., Jiang, H., Gu, B., and Chang, J.: Atmospheric reactive nitrogen in China: sources, recent trends, and damage costs, *Environ. Sci. Technol.*, 46, 9420–9427, 2012.

Guenther, A., Karl, T., Harley, P., Wiedinmyer, C., Palmer, P. I., and Geron, C.: Estimates of global terrestrial isoprene emissions using MEGAN (Model of Emissions of Gases and Aerosols from Nature), *Atmos. Chem. Phys.*, 6, 3181–3210, doi:10.5194/acp-6-3181-2006, 2006.

He, J., Balasubramanian, R., Burger, D. F., Hicks, K., Kuylenstierna, J. C., and Palani, S.: Dry and wet atmospheric deposition of nitrogen and phosphorus in Singapore, *Atmos. Environ.*, 45, 2760–2768, 2011.

Hennemuth, B. and Lammert, A.: Determination of the atmospheric boundary layer height from radiosonde and lidar backscatter, *Bound.-Lay. Meteorol.*, 120, 181–200, 2006.

Hoppel, W., Frick, G., and Fitzgerald, J.: Surface source function for sea-salt aerosol and aerosol dry deposition to the ocean surface, *J. Geophys. Res.-Atmos.*, 107, AAC 7-1–AAC 7-17, doi:10.1029/2001JD002014, 2002.

Discussion Paper | Discussion Paper

Title Page

Abstract

Introduction

Conclusions

References

Tables

Figures

|◀

▶|

◀

▶

Back

Close

Full Screen / Esc

Printer-friendly Version

Interactive Discussion



Hsu, S. C., Liu, S. C., Huang, Y. T., Lung, S. C. C., Tsai, F., Tu, J. Y., and Kao, S. J.: A criterion for identifying Asian dust events based on AI concentration data collected from northern Taiwan between 2002 and early 2007, *J. Geophys. Res.-Atmos.*, 113, D18306, doi:10.1029/2007JD009574, 2008.

Hsu, S.-C., Liu, S. C., Huang, Y.-T., Chou, C. C. K., Lung, S. C. C., Liu, T.-H., Tu, J.-Y., and Tsai, F.: Long-range southeastward transport of Asian biosmoke pollution: signature detected by aerosol potassium in Northern Taiwan, *J. Geophys. Res.*, 114, D18306, doi:10.1029/2007JD009574, doi:10.1029/2009jd011725, 2009.

Hsu, S., Liu, S., Tsai, F., Engling, G., Lin, I., Chou, C., Kao, S., Lung, S., Chan, C., and Lin, S.: High wintertime particulate matter pollution over an offshore island (Kinmen) off southeastern China: an overview, *J. Geophys. Res.-Atmos.*, 115, D17309, doi:10.1029/2009JD013641, 2010a.

Hsu, S.-C., Wong, G. T. F., Gong, G.-C., Shiah, F.-K., Huang, Y.-T., Kao, S.-J., Tsai, F., Candice Lung, S.-C., Lin, F.-J., Lin, I. I., Hung, C.-C., and Tseng, C.-M.: Sources, solubility, and dry deposition of aerosol trace elements over the East China Sea, *Mar. Chem.*, 120, 116–127, doi:10.1016/j.marchem.2008.10.003, 2010b.

Hsu, S. C., Lee, C. S. L., Huh, C. A., Shaheen, R., Lin, F. J., Liu, S. C., Liang, M. C., and Tao, J.: Ammonium deficiency caused by heterogeneous reactions during a super Asian dust episode, *J. Geophys. Res.-Atmos.*, 119, 6803–6817, 2014.

Husar, R. B., Tratt, D., Schichtel, B. A., Falke, S., Li, F., Jaffe, D., Gasso, S., Gill, T., Laulainen, N. S., and Lu, F.: Asian dust events of April 1998, *J. Geophys. Res.-Atmos.*, 106, 18317–18330, 2001.

Jickells, T., Kelly, S., Baker, A., Biswas, K., Dennis, P., Spokes, L., Witt, M., and Yeatman, S.: Isotopic evidence for a marine ammonia source, *Geophys. Res. Lett.*, 30, 1374, doi:10.1029/2002GL016728, 2003.

Jickells, T., An, Z., Andersen, K. K., Baker, A., Bergametti, G., Brooks, N., Cao, J., Boyd, P., Duce, R., and Hunter, K.: Global iron connections between desert dust, ocean biogeochemistry, and climate, *Science*, 308, 67–71, doi:10.1126/science.1105959, 2005.

Jickells, T., Baker, A., Cape, J., Cornell, S., and Nemitz, E.: The cycling of organic nitrogen through the atmosphere, *Philos. T. R. Soc. B*, 368, 20130115, doi:10.1098/rstb.2013.0115, 2013.

Nitrogen speciation in various types of aerosol in spring over the northwestern Pacific Ocean

L. Luo et al.

[Title Page](#)

[Abstract](#)

[Introduction](#)

[Conclusions](#)

[References](#)

[Tables](#)

[Figures](#)

◀

▶

[Back](#)

[Close](#)

[Full Screen / Esc](#)

[Printer-friendly Version](#)

[Interactive Discussion](#)

5 Jung, J., Furutani, H., and Uematsu, M.: Atmospheric inorganic nitrogen in marine aerosol and precipitation and its deposition to the North and South Pacific Oceans, *J. Atmos. Chem.*, 68, 157–181, doi:10.1007/s10874-012-9218-5, 2011.

10 Jung, J., Furutani, H., Uematsu, M., Kim, S., and Yoon, S.: Atmospheric inorganic nitrogen input via dry, wet, and sea fog deposition to the subarctic western North Pacific Ocean, *Atmos. Chem. Phys.*, 13, 411–428, doi:10.5194/acp-13-411-2013, 2013.

15 Kanakidou, M., Duce, R. A., Prospero, J. M., Baker, A. R., Benitez-Nelson, C., Dentener, F. J., Hunter, K. A., Liss, P. S., Mahowald, N., and Okin, G. S.: Atmospheric fluxes of organic N and P to the global ocean, *Global Biogeochem. Cy.*, 26, GB3026, doi:10.1029/2011GB004277, 2012.

20 Kang, C.-H., Kim, W.-H., Ko, H.-J., and Hong, S.-B.: Asian dust effects on total suspended particulate (TSP) compositions at Gosan in Jeju Island, Korea, *Atmos. Res.*, 94, 345–355, 2009.

25 Kang, J., Cho, B. C., and Lee, C.-B.: Atmospheric transport of water-soluble ions NO_3^- , NH_4^+ and nss- SO_4^{2-} to the southern East Sea (Sea of Japan), *Sci. Total Environ.*, 408, 2369–2377, 2010.

Kim, I.-N., Lee, K., Gruber, N., Karl, D. M., Bullister, J. L., Yang, S., and Kim, T.-W.: Increasing anthropogenic nitrogen in the North Pacific Ocean, *Science*, 346, 1102–1106, 2014.

20 Kim, T.-W., Lee, K., Najjar, R. G., Jeong, H.-D., and Jeong, H. J.: Increasing N abundance in the northwestern Pacific Ocean due to atmospheric nitrogen deposition, *Science*, 334, 505–509, 2011.

Knapp, A. N., Sigman, D. M., and Lipschultz, F.: N isotopic composition of dissolved organic nitrogen and nitrate at the Bermuda Atlantic Time-series Study site, *Global Biogeochem. Cy.*, 19, GB1018, doi:10.1029/2004GB002320, 2005.

25 Knapp, A. N., Sigman, D. M., Lipschultz, F., Kustka, A. B., and Capone, D. G.: Inter-basin isotopic correspondence between upper-ocean bulk DON and subsurface nitrate and its implications for marine nitrogen cycling, *Global Biogeochem. Cy.*, 25, GB4004, doi:10.1029/2010GB003878, 2011.

30 Kundu, S., Kawamura, K., and Lee, M.: Seasonal variation of the concentrations of nitrogenous species and their nitrogen isotopic ratios in aerosols at Gosan, Jeju Island: implications for atmospheric processing and source changes of aerosols, *J. Geophys. Res.-Atmos.*, 115, D20305, doi:10.1029/2009JD013323, 2010.

Title Page

Abstract

Introduction

Conclusions

References

Tables

Figures

◀

▶

◀

▶

Back

Close

Full Screen / Esc

Printer-friendly Version

Interactive Discussion

5 Lange, C. A., Matschullat, J., Zimmermann, F., Sterzik, G., and Wienhaus, O.: Fog frequency and chemical composition of fog water – a relevant contribution to atmospheric deposition in the Eastern Erzgebirge, Germany, *Atmos. Environ.*, 37, 3731–3739, 2003.

10 Lesworth, T., Baker, A. R., and Jickells, T.: Aerosol organic nitrogen over the remote Atlantic Ocean, *Atmos. Environ.*, 44, 1887–1893, 2010.

15 Li, X. A., Yu, Z., Song, X., Cao, X., and Yuan, Y.: Nitrogen and phosphorus budgets of the Changjiang River estuary, *Chin. J. Oceanol. Limn.*, 29, 762–774, 2011.

20 Liu, X., Penner, J. E., and Herzog, M.: Global modeling of aerosol dynamics: model description, evaluation, and interactions between sulfate and nonsulfate aerosols, *J. Geophys. Res.-Atmos.*, 110, D18206, doi:10.1029/2004JD005674, 2005.

25 Mace, K. A., Duce, R. A., and Tindale, N. W.: Organic nitrogen in rain and aerosol at Cape Grim, Tasmania, Australia, *J. Geophys. Res.-Atmos.*, 108, 4338, doi:10.1029/2002JD003051, 2003a.

30 Mace, K. A., Kubilay, N., and Duce, R. A.: Organic nitrogen in rain and aerosol in the eastern Mediterranean atmosphere: an association with atmospheric dust, *J. Geophys. Res.-Atmos.*, 108, 4320, doi:10.1029/2002JD002997, 2003b.

Maria, S. F. and Russell, L. M.: Organic and inorganic aerosol below-cloud scavenging by suburban New Jersey precipitation, *Environ. Sci. Technol.*, 39, 4793–4800, 2005.

35 Miyazaki, Y., Kawamura, K., Jung, J., Furutani, H., and Uematsu, M.: Latitudinal distributions of organic nitrogen and organic carbon in marine aerosols over the western North Pacific, *Atmos. Chem. Phys.*, 11, 3037–3049, doi:10.5194/acp-11-3037-2011, 2011.

40 Moore, K. F., Sherman, D. E., Reilly, J. E., Hannigan, M. P., Lee, T., and Collett, J. L.: Drop size-dependent chemical composition of clouds and fogs. Part II: Relevance to interpreting the aerosol/trace gas/fog system, *Atmos. Environ.*, 38, 1403–1415, 2004.

45 Nakamura, T., Matsumoto, K., and Uematsu, M.: Chemical characteristics of aerosols transported from Asia to the East China Sea: an evaluation of anthropogenic combined nitrogen deposition in autumn, *Atmos. Environ.*, 39, 1749–1758, 2005.

50 Nakamura, T., Ogawa, H., Maripi, D. K., and Uematsu, M.: Contribution of water soluble organic nitrogen to total nitrogen in marine aerosols over the East China Sea and western North Pacific, *Atmos. Environ.*, 40, 7259–7264, 2006.

55 Reis, S., Pinder, R. W., Zhang, M., Lijie, G., and Sutton, M. A.: Reactive nitrogen in atmospheric emission inventories, *Atmos. Chem. Phys.*, 9, 7657–7677, doi:10.5194/acp-9-7657-2009, 2009.

Nitrogen speciation in various types of aerosol in spring over the northwestern Pacific Ocean

L. Luo et al.

[Title Page](#)[Abstract](#)[Introduction](#)[Conclusions](#)[References](#)[Tables](#)[Figures](#)[|◀](#)[▶|](#)[Back](#)[Close](#)[Full Screen / Esc](#)[Printer-friendly Version](#)[Interactive Discussion](#)

**Nitrogen speciation
in various types of
aerosol in spring over
the northwestern
Pacific Ocean**

L. Luo et al.

Sasakawa, M. and Uematsu, M.: Chemical composition of aerosol, sea fog, and rainwater in the marine boundary layer of the northwestern North Pacific and its marginal seas, *J. Geophys. Res.-Atmos.*, 107, ACH 17-11–ACH 17-19, 2002.

Sasakawa, M. and Uematsu, M.: Relative contribution of chemical composition to acidification of sea fog (stratus) over the northern North Pacific and its marginal seas, *Atmos. Environ.*, 39, 1357–1362, 2005.

Savoie, D. and Prospero, J.: Water-soluble potassium, calcium, and magnesium in the aerosols over the tropical North Atlantic, *J. Geophys. Res.-Oceans*, 85, 385–392, 1980.

Shao, Y. and Dong, C.: A review on East Asian dust storm climate, modelling and monitoring, *Global Planet. Change*, 52, 1–22, 2006.

Shi, G., Li, Y., Jiang, S., An, C., Ma, H., Sun, B., and Wang, Y.: Large-scale spatial variability of major ions in the atmospheric wet deposition along the China Antarctica transect (31° N–69° S), *Tellus B*, 64, 1–10, 2012.

Shi, J., Gao, H., Qi, J., Zhang, J., and Yao, X.: Sources, compositions, and distributions of water-soluble organic nitrogen in aerosols over the China Sea, *J. Geophys. Res.-Atmos.*, 115, D17303, doi:10.1029/2009JD013238, 2010.

Spokes, L. J. and Liss, P. S.: Photochemically induced redox reactions in seawater, II. Nitrogen and iodine, *Mar. Chem.*, 54, 1–10, 1996.

Srinivas, B., Sarin, M., and Sarma, V.: Atmospheric dry deposition of inorganic and organic nitrogen to the Bay of Bengal: impact of continental outflow, *Mar. Chem.*, 127, 170–179, 2011.

Sun, J., Zhang, M., and Liu, T.: Spatial and temporal characteristics of dust storms in China and its surrounding regions, 1960–1999: Relations to source area and climate, *J. Geophys. Res.-Atmos.*, 106, 10325–10333, 2001.

Uematsu, M., Hattori, H., Nakamura, T., Narita, Y., Jung, J., Matsumoto, K., Nakaguchi, Y., and Kumar, M. D.: Atmospheric transport and deposition of anthropogenic substances from the Asia to the East China Sea, *Mar. Chem.*, 120, 108–115, 2010.

Violaki, K., Zarbas, P., and Mihalopoulos, N.: Long-term measurements of dissolved organic nitrogen (DON) in atmospheric deposition in the Eastern Mediterranean: fluxes, origin and biogeochemical implications, *Mar. Chem.*, 120, 179–186, 2010.

Violaki, K., Sciare, J., Williams, J., Baker, A. R., Martino, M., and Mihalopoulos, N.: Atmospheric water-soluble organic nitrogen (WSON) over marine environments: a global perspective, *Bio-geosciences*, 12, 3131–3140, doi:10.5194/bg-12-3131-2015, 2015.

Discussion Paper | Discussion Paper

Discussion Paper | Discussion Paper

[Title Page](#)

[Abstract](#)

[Introduction](#)

[Conclusions](#)

[References](#)

[Tables](#)

[Figures](#)

[|◀](#)

[▶|](#)

[◀](#)

[▶](#)

[Back](#)

[Close](#)

[Full Screen / Esc](#)

[Printer-friendly Version](#)

[Interactive Discussion](#)



5 Vione, D., Maurino, V., Minero, C., and Pelizzetti, E.: Reactions induced in natural waters by irradiation of nitrate and nitrite ions, in: Environmental Photochemistry Part II, Springer, 221–253, 2005.

10 Wedyan, M., Fandi, K., and Al-Rousan, S.: Bioavailability of atmospheric dissolved organic nitrogen in the marine aerosol over the Gulf of Aqaba, *Australian J. Basic Appl. Sci.*, 1, 208–212, 2007.

15 Xie, H., Bélanger, S., Song, G., Benner, R., Taalba, A., Blais, M., Tremblay, J.-É., and Babin, M.: Photoproduction of ammonium in the southeastern Beaufort Sea and its biogeochemical implications, *Biogeosciences*, 9, 3047–3061, doi:10.5194/bg-9-3047-2012, 2012.

20 10 Yan, G. and Kim, G.: Sources and fluxes of organic nitrogen in precipitation over the southern East Sea/Sea of Japan, *Atmos. Chem. Phys.*, 15, 2761–2774, doi:10.5194/acp-15-2761-2015, 2015.

25 Yao, X. H. and Zhang, L.: Supermicron modes of ammonium ions related to fog in rural atmosphere, *Atmos. Chem. Phys.*, 12, 11165–11178, doi:10.5194/acp-12-11165-2012, 2012.

30 15 Yue, Y., Niu, S., Zhao, L., Zhang, Y., and Xu, F.: Chemical Composition of Sea Fog Water Along the South China Sea, *Pure Appl. Geophys.*, 169, 2231–2249, doi:10.1007/s00024-012-0486-4, 2012.

35 Yue, Y., Niu, S., Zhao, L., Zhang, Y., and Xu, F.: The influences of macro-and microphysical characteristics of sea-fog on fog-water chemical composition, *Adv. Atmos. Sci.*, 31, 624–636, 2014.

40 Zamora, L., Prospero, J., and Hansell, D.: Organic nitrogen in aerosols and precipitation at Barbados and Miami: Implications regarding sources, transport and deposition to the western subtropical North Atlantic, *J. Geophys. Res.-Atmos.*, 116, D20309, doi:10.1029/2011JD015660, 2011.

45 25 Zhang, G., Zhang, J., and Liu, S.: Characterization of nutrients in the atmospheric wet and dry deposition observed at the two monitoring sites over Yellow Sea and East China Sea, *J. Atmos. Chem.*, 57, 41–57, 2007.

50 Zhang, R., Jing, J., Tao, J., Hsu, S.-C., Wang, G., Cao, J., Lee, C. S. L., Zhu, L., Chen, Z., Zhao, Y., and Shen, Z.: Chemical characterization and source apportionment of $PM_{2.5}$ in Beijing: seasonal perspective, *Atmos. Chem. Phys.*, 13, 7053–7074, doi:10.5194/acp-13-7053-2013, 2013.

Nitrogen speciation in various types of aerosol in spring over the northwestern Pacific Ocean

L. Luo et al.

[Title Page](#)

[Abstract](#)

[Introduction](#)

[Conclusions](#)

[References](#)

[Tables](#)

[Figures](#)

[|◀](#)

[▶|](#)

[◀](#)

[▶](#)

[Back](#)

[Close](#)

[Full Screen / Esc](#)

[Printer-friendly Version](#)

[Interactive Discussion](#)

Zhang, S.-P., Xie, S.-P., Liu, Q.-Y., Yang, Y.-Q., Wang, X.-G., and Ren, Z.-P.: Seasonal Variations of Yellow Sea Fog: observations and Mechanisms*, *J. Climate*, 22, 6758–6772, doi:10.1175/2009jcli2806.1, 2009.

Zhang, Y., Song, L., Liu, X., Li, W., Lü, S., Zheng, L., Bai, Z., Cai, G., and Zhang, F.: Atmospheric organic nitrogen deposition in China, *Atmos. Environ.*, 46, 195–204, 2012.

Zhu, L., Chen, Y., Guo, L., and Wang, F.: Estimate of dry deposition fluxes of nutrients over the East China Sea: the implication of aerosol ammonium to non-sea-salt sulfate ratio to nutrient deposition of coastal oceans, *Atmos. Environ.*, 69, 131–138, doi:10.1016/j.atmosenv.2012.12.028, 2013.

Nitrogen speciation in various types of aerosol in spring over the northwestern Pacific Ocean

L. Luo et al.

[Title Page](#)

[Abstract](#)

[Introduction](#)

[Conclusions](#)

[References](#)

[Tables](#)

[Figures](#)

◀

▶

[Back](#)

[Close](#)

[Full Screen / Esc](#)

[Printer-friendly Version](#)

[Interactive Discussion](#)



Table 1. Nitrogen speciation in various aerosols from different reported regions.

Sample type	Date	Location		NO_3^- nmol m ⁻³	NH_4^+ nmol m ⁻³	WSON nmol m ⁻³	NO_3^- % ^a	NH_4^+ % ^a	WSON % ^a	Reference
TSP (Fog)	Mar–Apr 2014	ECSs	Shelf	536 ± 300	442 ± 194	147 ± 171	48 ± 7	42 ± 9	10 ± 6	This study
TSP (Dust)	Mar–Apr 2014	NWPO	Remote ocean	100 ± 23	138 ± 24	11.2 ± 4.0	41 ± 5	56 ± 7	5 ± 2	This study
TSP (Bgd.)	Mar–Apr 2014	NWPO	Remote ocean	26 ± 32	54 ± 45	10.9 ± 6.8	27 ± 9	60 ± 11	14 ± 8	This study
TSP (Dust)	Aug–Sep 2007, 2008	Barbados, Atlantic	Island	101 ± 4	11 ± 7	1.4 ± 1.3	45 ^c	49 ^c	6 ^c	Zamora et al. (2011)
TSP (Dust)	May 2007–Jul 2009	Miami, FL, Atlantic	Coast city	28 ± 9	26 ± 10	3.0 ± 2.0	50 ^c	45 ^c	5 ^c	Violaki et al. (2015)
$\text{PM}_{2.5}$ (Dust)		Tropic Atlantic Ocean							14	Violaki et al. (2015)
TSP (Dust)	Mar 2005–Apr 2007	Southwest ECS	Shelf	84 ± 98	177 ± 151	–	–	–	–	Hsu et al. (2010b)
TSP (Dust)	Feb 1992–May 2004	Island of Jeju	Island	71 ± 44	72 ± 48	–	–	–	–	Kang et al. (2009)
TSP	Feb–Mar 2007	Northwest ECS	Shelf	68 ^c	193 ^c	–	–	–	–	Shi et al. (2010)
TSP	Mar 2005–Apr 2007	Southwest ECS	Shelf	38 ± 45	89 ± 76	–	–	–	–	Hsu et al. (2010b)
TSP	Sep–Oct 2002	ECS	Shelf	34 ^c	136 ^c	54 ± 36	15 ^c	61 ^c	24	Nakamura et al. (2006)
TSP	Mar 2004	ECS	Shelf	39 ^c	91 ^c	16 ± 19	27 ^c	62 ^c	10	
TSP	Mar 2005, Apr 2006	Yellow sea	Shelf	–	–	–	–	–	20	Shi et al. (2010)
TSP	Apr 2010	Northwest ECS	Island	111 ^c	76 ^c	–	–	–	–	Zhu et al. (2013)
TSP	Mar 2011	Northwest ECS	Island	137 ^c	202 ^c	–	–	–	–	Zhu et al. (2013)
TSP	Spring 2003–2004	Northeast ECS	Island	35 ± 19	50 ± 28	–	–	–	–	Kundu et al. (2010)
TSP	Jul–Aug 2008	NWPO	Remote ocean	2.5	5.6	–	–	–	–	Jung et al. (2013)
TSP	Aug 2003–Sep 2005	Gulf of Aqaba	Coast	39 ± 19	25 ± 14	8 ± 5	53 ^c	34 ^c	11 ^c	Chen et al. (2007)
TSP	Nov–Dec 2000	Island of Tasmania	Island	11 ± 7	2.6 ± 3.0	3.6 ± 5.7	63	15	21	Mace et al. (2003a)
TSP	Aug–Sep 2008	NWP	Remote ocean	1.8 ± 1.5	1.2 ± 1.1	1.1 ± 0.93	43 ^c	30 ^c	28 ^c	Miyazaki et al. (2011)
TSP	Apr 2007–Mar 2008	Marina, Singapore	urban	50 ± 31	14 ± 8	56 ± 22	40 ± 15	11 ± 6	49 ± 17	He et al. (2011)
TSP	Jan–Dec 2006	Keelung, Taiwan	Coast city			76 ± 28			26 ^c	Chen et al. (2010)
TSP (Sea-spray)				6.7 ± 2.7	4.2 ± 1.7	0.5 ± 0.3	59 ^c	37 ^c	4 ^c	Zamora et al. (2011)
TSP (Bb) ^b				11 ± 11	18 ± 13	3.3 ± 2.0	34 ^c	56 ^c	10 ^c	
TSP (Bb) ^b				28 ± 16	48 ± 48	6.2 ± 6.4	34 ^c	58 ^c	8 ^c	Zamora et al. (2011)
TSP (Pollution)				22 ± 11	23 ± 24	3.7 ± 2.8	45 ^c	48 ^c	8 ^c	
$\text{PM}_{1.3-10}$	2005, 2006	Crete, Greece	Island	26 ± 9	8.9 ± 4.0	5.5 ± 3.9	64	23	13	Violaki et al. (2010)
PM_1	2005, 2006	Crete, Greece		1.5 ± 1.3	70 ± 35	12 ± 14	2	85	13	
$\text{PM}_{2.5}$	Jan–Dec 2005	Indian Ocean	Remote ocean	0.3 ± 0.2	1.3 ± 1.0	0.8 ± 1.4	14	53	32	Violaki et al. (2015)
$\text{PM}_{2.5-10}$				0.2 ± 0.1	0.3 ± 0.1	0.2 ± 0.4	26	39	35	
$\text{PM}_{2.5}$	Jan–Feb 2007	Middle S. Atlantic	Remote ocean			1.1 1.2			43	

^a Percent in total dissolved nitrogen.^b Bb indicated Biomass burning.^c Calculated value from the original data.

Nitrogen speciation in various types of aerosol in spring over the northwestern Pacific Ocean

L. Luo et al.

[Title Page](#)[Abstract](#)[Introduction](#)[Conclusions](#)[References](#)[Tables](#)[Figures](#)[|◀](#)[▶|](#)[Back](#)[Close](#)[Full Screen / Esc](#)[Printer-friendly Version](#)[Interactive Discussion](#)

Nitrogen speciation in various types of aerosol in spring over the northwestern Pacific Ocean

L. Luo et al.

[Title Page](#)

[Abstract](#)

[Introduction](#)

[Conclusions](#)

[References](#)

[Tables](#)

[Figures](#)

◀

▶

[Back](#)

[Close](#)

[Full Screen / Esc](#)

[Printer-friendly Version](#)

[Interactive Discussion](#)

Table 2. Mean molar concentrations (nmol m^{-3}) of major ionic species and Al (ng m^{-3}) in sea fog modified aerosols and dust aerosols in the ECSSs.

	Sea fog ^a mean \pm SD	Dust ^b mean \pm SD	Dust ^c mean \pm SD
Na^+	123.2 ± 97.5	294.8 ± 238.3	130.4 ± 85.2
NH_4^+	441.5 ± 193.9	177.6 ± 150.7	72.2 ± 47.7
Mg^{2+}	24.1 ± 16.5	41.2 ± 32.4	25.0 ± 12.9
K^+	17.5 ± 9.9	21.8 ± 19.1	17.9 ± 9.2
Ca^{2+}	54.7 ± 52.2	61.7 ± 39.5	76.9 ± 58.5
Cl^-	125.2 ± 111.3	280.9 ± 349.1	121.3 ± 101.6
NO_3^-	535.9 ± 299.7	83.6 ± 98.4	71.0 ± 43.5
SO_4^{2-}	172.5 ± 54.1	145.2 ± 103.2	104.0 ± 47.2
nss- SO_4^{2-}	165.1 ± 50.3	94.9 ± 89.0	96.1 ± 47.3
Total Al	2460 ± 2160	3470 ± 2730	4900 ± 6500
Soluble Al	124 ± 36	38 ± 45	nd.
relative acidity	0.73 ± 0.13	1.07	1.06

^a This study; ^b Hsu et al. (2010b); ^c Kang et al. (2009)

Nitrogen speciation in various types of aerosol in spring over the northwestern Pacific Ocean

L. Luo et al.

Table 3. The depositional fluxes reported or calculated for the Asian region and Pacific Ocean based on assumed deposition velocity.

Locations	Collection type	Date	NO_3^- ^a	NH_4^+ ^a	WSON ^a	Total ^a	Reference
ECSs (Sea fog)	Cruise	Mar–Apr 2014	926 ± 518	38 ± 17	127 ± 148	1090 ± 671	This study
NWPO (Dust)	Cruise	Mar–Apr 2014	172 ± 40	11.9 ± 2.1	6.5 ± 5.7	190 ± 41.6	This study
NWPO (Bgd.)	Cruise	Mar–Apr 2014	44.6 ± 55.3	4.66 ± 3.90	7.6 ± 6.5	56.8 ± 59.1	This study
Subarctic western North Pacific	Cruise	Jul–Aug 2008	3.3 ± 2.3	1.9 ± 0.63	–	5.3 ± 2.6	Jung et al. (2011)
Subtropical western North Pacific	Cruise	Aug–Sep 2008	3.0 ± 1.5	2.7 ± 2.1	–	5.7 ± 3.5	Jung et al. (2011)
Central North Pacific	Cruise	Jan 2009	1.6 ± 0.44	1.4 ± 0.96	–	3.1 ± 1.4	Jung et al. (2011)
Northwest ECS*	Cruise	Feb–Mar 2007	117	17	–	134	Shi et al. (2010)
Southwest ECS*	Cruise	Spring 2005–2007	66	8	–	74	Hsu et al. (2010b)
Northwest ECS*	Coastal island	Apr 2010	192	6.6	–	198.6	Zhu et al. (2013)
Northwest ECS*	Coastal island	Mar 2011	237	17.5	–	254.5	Zhu et al. (2013)

* recalculated fluxes based on assumed deposition velocity

^a in $\mu\text{mol N m}^{-2} \text{d}^{-1}$

Title Page	Abstract	Introduction
Conclusions	References	
Tables	Figures	
◀	▶	
◀	▶	
Back	Close	
Full Screen / Esc		
Printer-friendly Version		
Interactive Discussion		

Nitrogen speciation in various types of aerosol in spring over the northwestern Pacific Ocean

L. Luo et al.

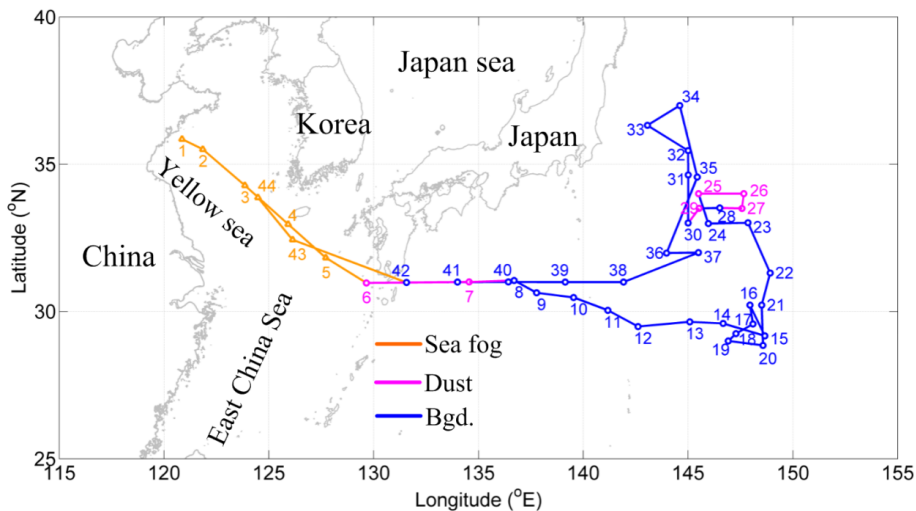


Figure 1. Map of the cruise track. Orange, pink and blue indicate sea fog, dust and background days during the cruise. Sample number and the collection range were shown.

- [Title Page](#)
- [Abstract](#) [Introduction](#)
- [Conclusions](#) [References](#)
- [Tables](#) [Figures](#)
- [◀](#) [▶](#)
- [◀](#) [▶](#)
- [Back](#) [Close](#)
- [Full Screen / Esc](#)
- [Printer-friendly Version](#)
- [Interactive Discussion](#)

Nitrogen speciation in various types of aerosol in spring over the northwestern Pacific Ocean

L. Luo et al.

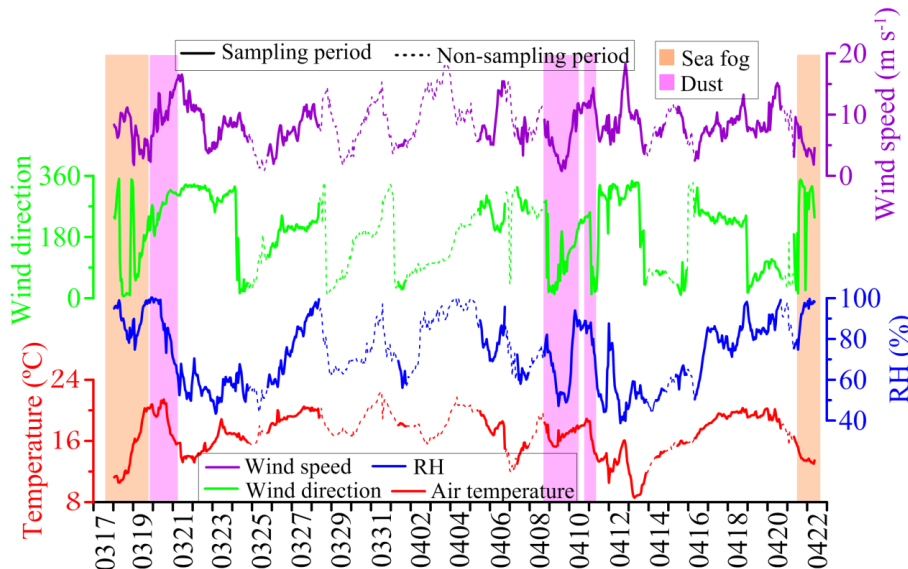


Figure 2. The meteorological parameters collected during the sampling period (solid line). Wind speed is in purple, wind direction in green, relative humidity (RH) in blue and temperature in red. Orange shade indicates the period of sea fog contact and pink indicates the dust period. Non-sampling period is in dashed curves.

Title Page	Abstract	Introduction
Conclusions	References	
Tables	Figures	
◀	▶	
◀	▶	
Back	Close	
Full Screen / Esc		
Printer-friendly Version		
Interactive Discussion		

Nitrogen speciation in various types of aerosol in spring over the northwestern Pacific Ocean

L. Luo et al.

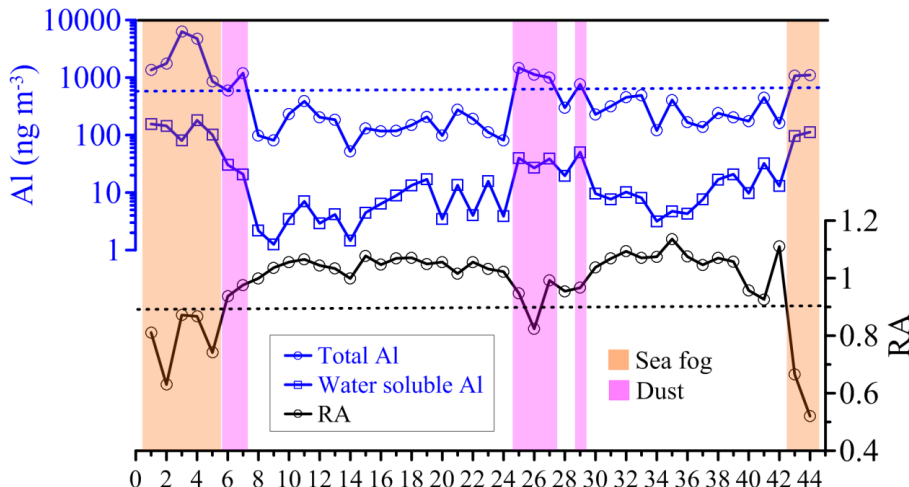


Figure 3. Total and water soluble Al concentrations and relative acidity (RA) for TSP. Orange bar indicates the sea fog period, pink bar indicates the dust period. Sample identifications are shown on x axis (see Table S1). The horizontal blue dashed line (590 ng m^{-3}) stands for the reference to define background aerosols, and black dashed line indicates the criterion of 0.9 for relative acidity.

Nitrogen speciation in various types of aerosol in spring over the northwestern Pacific Ocean

L. Luo et al.

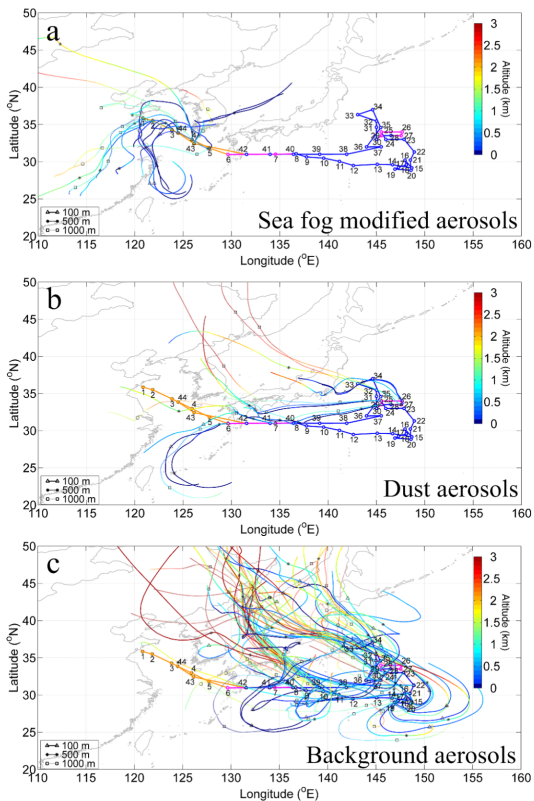


Figure 4. Map and cruise track superimposed on 3-day air mass back trajectories corresponding to each sample. Altitudes of 100 m (triangle), 500 m a.s.l. (asterisk) and 1000 m a.s.l. (square) during the collecteions of (a) sea fog modified aerosols, (b) dust aerosols and (c) background aerosols. Colour bar represents altitude (in km).

Nitrogen speciation in various types of aerosol in spring over the northwestern Pacific Ocean

L. Luo et al.

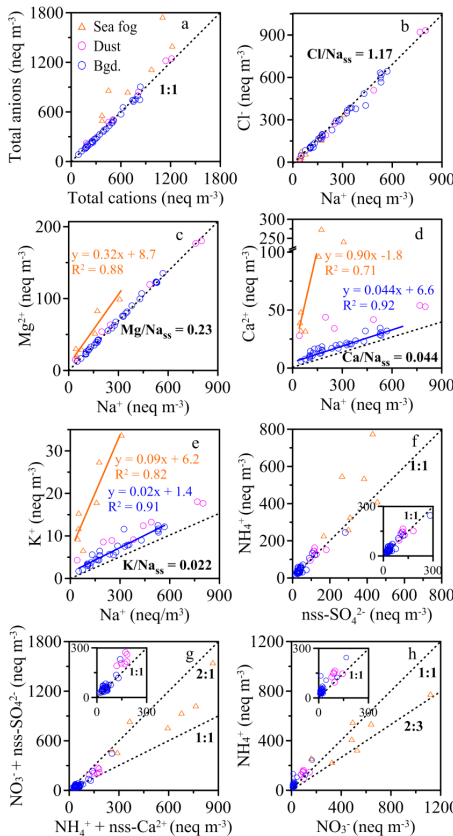


Figure 5. Scatter plots for equivalent concentrations of specific ions. **(a)** Total anions vs. total cations, **(b)** chloride vs. sodium, **(c)** magnesium vs. sodium, **(d)** calcium vs. sodium, **(e)** potassium vs. sodium, **(f)** ammonium vs. nss-sulfate, **(g)** $\sum(\text{nitrate} + \text{nss-sulfate})$ vs. $\sum(\text{nss-calcium} + \text{ammonium})$ and **(h)** nitrate vs. ammonium. Orange, pink and blue are for sea fog modified, dust and background aerosols, respectively.

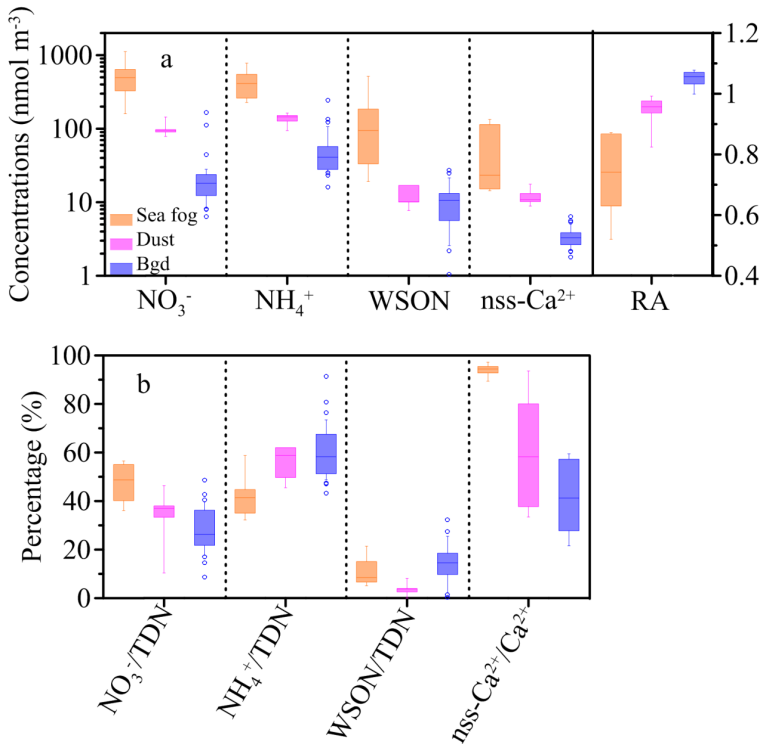


Figure 6. Box plots for **(a)** concentrations of NO_3^- , NH_4^+ , WSON and nss- Ca^{2+} , and RA, and **(b)** fractions of nitrogen species in total dissolved nitrogen and proportion of nss- Ca^{2+} in Ca^{2+} , in sea fog modified, dust and background aerosols. The large boxes represent the inter-quartile range from 25th to 75th percentile. The line inside the box indicates the median value. The whiskers extend upward to 90th and downward to 10th percentile.

Nitrogen speciation in various types of aerosol in spring over the northwestern Pacific Ocean

L. Luo et al.

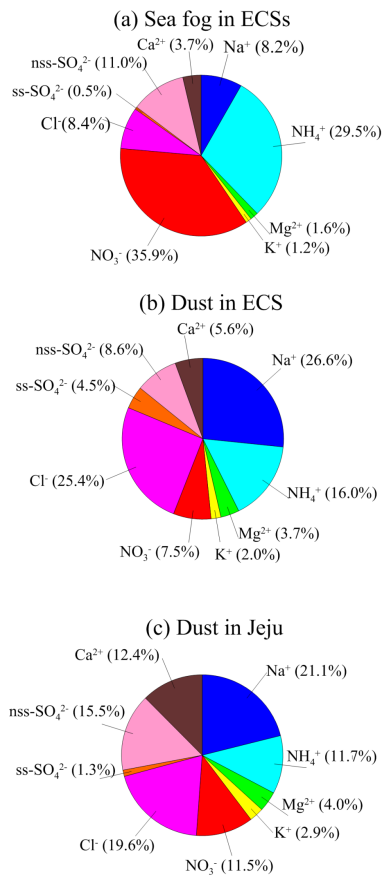


Figure 7. Pie charts of ion distribution for **(a)** sea fog modified aerosols (this study), **(b)** dust aerosols collected over the East China Sea ($n = 8$) (Hsu et al., 2010b), and **(c)** dust aerosols collected on the island of Jeju ($n = 49$) (Kang et al., 2009).

Nitrogen speciation in various types of aerosol in spring over the northwestern Pacific Ocean

L. Luo et al.

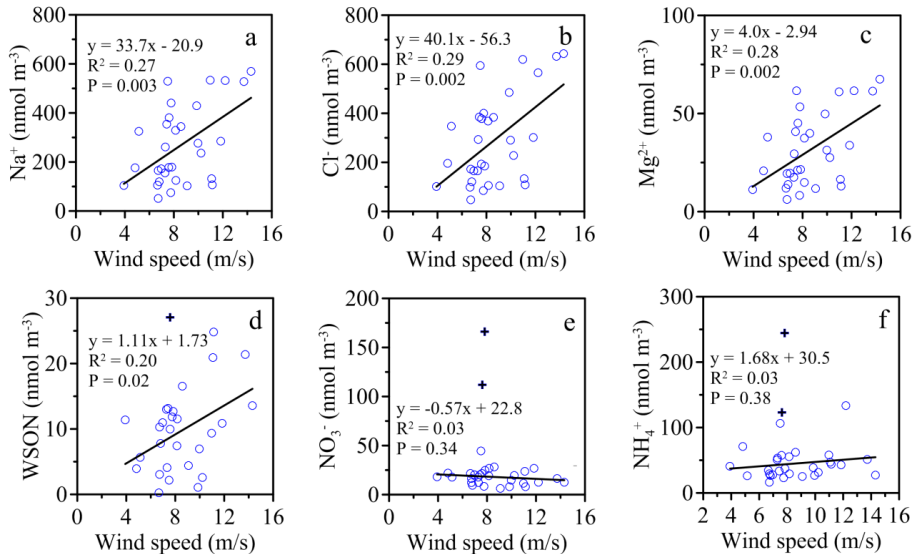


Figure 8. Scatter plots of concentrations of (a) Na^+ , (b) Cl^- , (c) Mg^{2+} , (d) WSON, (e) NO_3^- , (f) NH_4^+ against corresponding wind speed for background aerosols. Wind speed was derived by averaging wind speed (5 min average) in corresponding sampling intervals. Crosses in (d), (e) and (f) are not considered during linear regression.

Nitrogen speciation in various types of aerosol in spring over the northwestern Pacific Ocean

L. Luo et al.

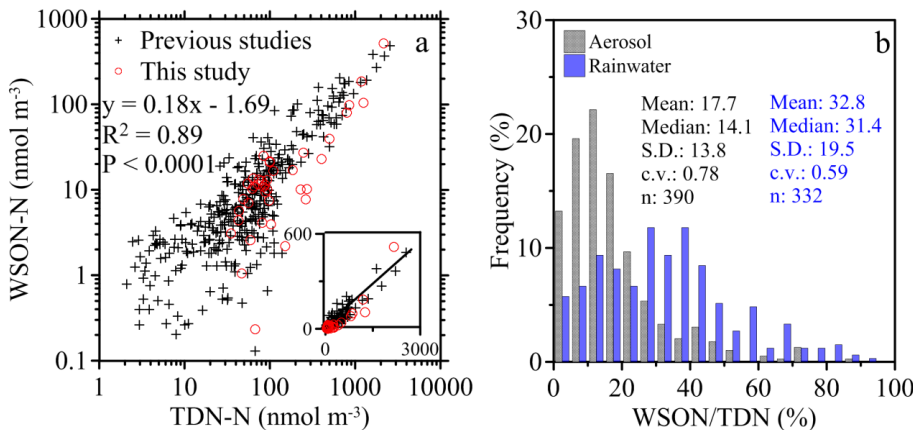


Figure 9. (a) Scatter plot of published aerosol WSON and total dissolve nitrogen (TDN) concentrations from the world (red circles for this study, black crosses from Lesworth et al., 2010; Chen et al., 2007; Mace et al., 2003a; Miyazaki et al., 2011; Shi et al., 2010; Srinivas et al., 2011; Zamora et al., 2011; Violaki et al., 2015). **(b)** Frequency histograms for percent WSON in aerosol TDN (grey bars, data from Fig. 9a) and in rainwater (blue bars, data from Cornell, 2011; Zhang et al., 2012; Altieri et al., 2012; Cui et al., 2014; Chen et al., 2015; Yan and Kim, 2015).

Title Page

Abstract

Introduction

Conclusions

References

Tables

Figures

1

1

Back

Close

Full Screen / Esc

Interactive Discussion

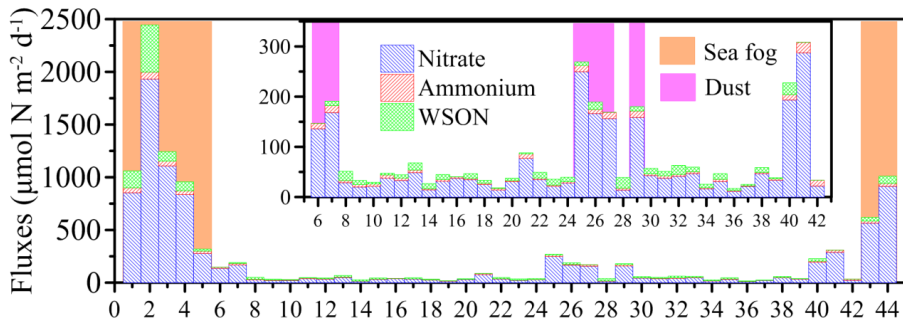


Figure 10. Dry deposition of aerosol nitrogen against sample identification. Nitrate is in blue, ammonium in red and WSON in green. Sample identifications, which match with Table S1, are shown on x axis.